International Journal of Bifurcation and Chaos, Vol. 15, No. 8 (2005) 2317–2348

ACTIVE WALKS: THE FIRST TWELVE YEARS (PART I)

LUI LAM
Department of Physics, San Jose State University,
San Jose, CA 95192-0106, USA
luilam@email.sjsu.edu

Received December 9, 2004

Active walk is a paradigm for self-organization and pattern formation in simple and complex systems, originated by Lam in 1992. In an active walk, the walker (an agent) changes the deformable landscape as it walks and is influenced by the changed landscape in choosing its next step. Active walk models have been applied successfully to various biological, chemical and physical systems from the natural sciences, and to economics and many other systems from the social sciences. More recently, it has been used to model human history. In this review, the history, basic concepts, formulation, theories, applications, new developments and open problems of active walk are summarized and discussed. New experimental, theoretical and computer modeling results are included.

Keywords: Active walk; active walker; agent-based modeling; pattern formation; complex system; dielectric breakdown.

Contents

1. The Birth of a Paradigm

I was shocked. Mireille, a young and intelligent researcher in liquid crystals at Orsay, had just passed away. Gone, forever, just like that.

The solid state lab at Orsay was established by Jacques Friedel and his friends. It was here that Pierre de Gennes led an army of French scientists and beat out the competition in the field of liquid crystals. Orsay is also the place that I worked briefly as a visitor in 1980 and 1982, when I was a member of the Institute of Physics, Chinese Academy of Sciences, in Beijing. When I heard the news about Mireille from one of my many good friends in Orsay, in the summer of 1987, I was visiting the institution on my way to a liquid crystal polymer conference at Bordeaux, France, from my home in New York City. (See [Lam, 1988].) After shock, came sadness and disappointment. The liquid crystal community was relatively small and the practitioners met every two years for a conference; it is almost like a family. How did I, a colleague in the same field, not know Mireille's death until I arrived at Orsay, almost by accident? It became clear to me that the liquid crystal community should be organized better and have a publication similar to *Physics Today*. And so, I decided to establish an international liquid crystal society. But it was not that easy.

In the next three years, I mentioned the idea to every liquid crystal friend, circulated a petition for support around the globe, pushed the proposal through the existing power structure — The Planning and Steering Committee for International Liquid Crystal Conferences, and wrote the bylaws. In the bylaws, I named it the "International Liquid Crystal Society" and made sure the society would publish an official magazine called *Liquid Crystals Today*. Finally, in the summer of 1990, everything was ready. I proposed to found the new society during the upcoming "13th International Liquid Crystal Conference" in Vancouver, Canada. And so I had to make a trip to Vancouver. But there was a problem. I was scheduled to present a paper at that conference but I did not yet have enough material to write this paper.

It turned out that 1990 was a busy year for me. In January, I organized a "Winter School in Nonlinear Physics" at San Jose State University. In March, in Anaheim, California, I chaired the American Physical Society Symposium on "Instabilities and Propagating Patterns in Soft Matter Physics," which I originally proposed. In June I was the Director of the NATO Advanced Research Workshop on "Nonlinear Dynamical Structures in Simple and Complex Liquids," in Los Alamos. This was followed in July by a "Nonlinear and Chaotic Phenomena" conference in Edmonton, Canada, a few days before the liquid crystal conference in Vancouver. (See [Lam, 1991].)

It was a few days before this conference in Edmonton that we rushed through a simple experiment in our "Nonlinear Physics Laboratory" at San Jose State University, in Room 55 in the basement of the Science Building. The experiment was so simple that it could be finished in less than one second. What we did was take a liquid crystal cell — a thin layer of liquid crystal between two conductive, transparent glass plates (the same one you would find in any digital watch or calculator), put in

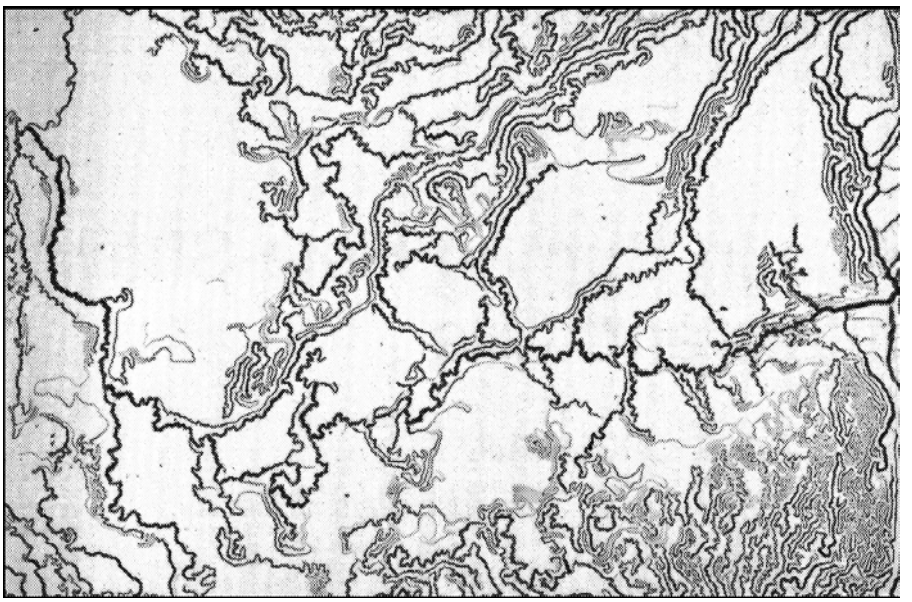

(a)

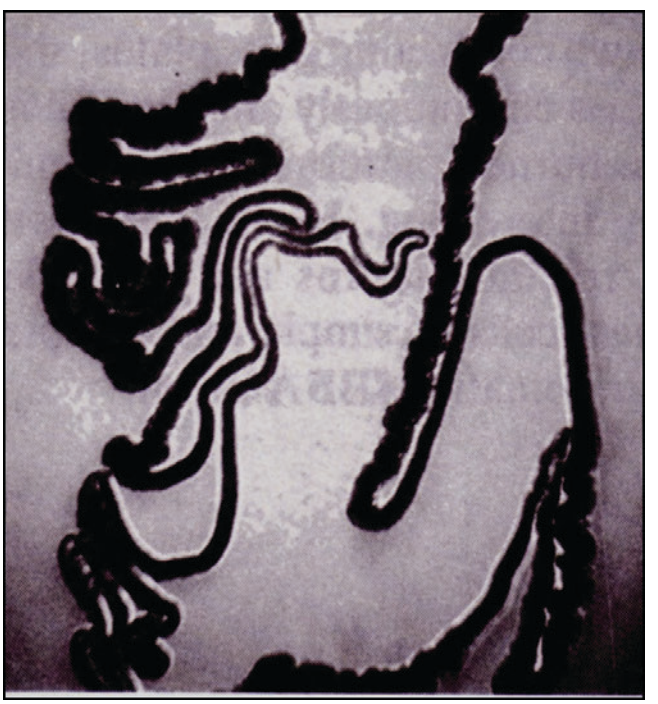

(b)

Fig. 1. A surface-reaction filamentary pattern induced by dielectric breakdown [Lam *et al.*, 1991]. (a) The pattern in a uniform oil cell. (b) A partial blow up of (a), showing the intermittent variation of filament width.

liquid crystal or oil, and apply a high enough voltage across the cell. After a flash of light, the experiment was finished and we found a complicated filamentary pattern left on the inner surfaces of the coated glass plates. An example is shown in Fig. 1. I wrote up the paper right before I rushed to the airport, and later presented these results in Vancouver [Lam *et al.*, 1991].

The physical and chemical processes giving rise to these filaments are rather complicated, and are still being investigated. Essentially, the filaments are the locations for a series of chemical reactions

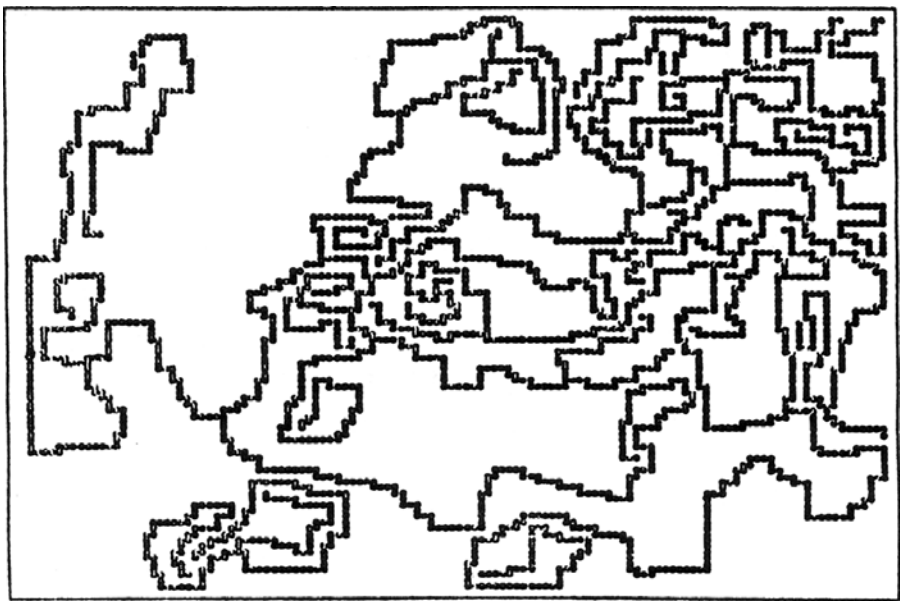

Fig. 2. Simulation from an active walk model [Freimuth & Lam, 1992]. Seven active walkers, placed initially at random locations, walk according to the PAW rule without branching. They influence each other indirectly through the shared, deformable landscape (not shown here). The built in noncrossing of tracks ensures that pockets of empty space of varying sizes are created, like that observed in experiments (see Fig. 1).

induced by dielectric breakdown. After this experiment, without knowledge of the physical mechanisms, we set out to do a computer modeling of this filamentary pattern. We soon realized that a growing filament could be identified as the track of a walker. To grow the filament, we only have to tell the walker how to walk, and specify how the walker changes the local environment as it walks. One of our computer results presented in Fig. 2, agrees fairly well with the experiment in Fig. 1. When I wrote up the paper for my 1992 book, *Modeling Complex Phenomena*, I named the walkers "active walkers" and the model the "active walker model" [Freimuth & Lam, 1992]. Subsequently, I called the process an "active walk" (AW) and started to refer to these models as "active walk models" [Lam, 1994]. And quite immediately, I realized that AW is not just good for modeling filament growth, but is in fact a general paradigm applicable to many other complex systems [Lam & Pochy, 1993].

"Physics of Pattern Formation in Complex Dissipative Systems," the international conference held in Kitakyushu, Japan, in September 1991, was the first occasion that I presented AW outside of San Jose [Lam *et al.*, 1992]. The next year, I talked about AW in three other international conferences — in Los Alamos in May, Edmonton in June, and Hamburg, Germany, in July. It was at this Los Alamos conference [Pochy *et al.*, 1993] that Harvey Gould invited me to write a review — the first review ever on AW, which was then barely one

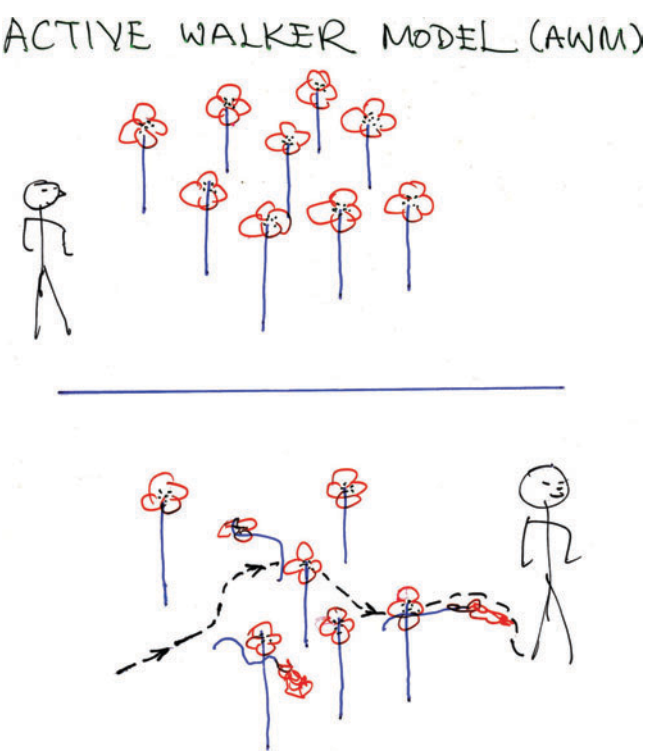

Fig. 3. The "active walker model" transparency presented in Hamburg, 1992. The walker alters the environment, the flowers, as he walks and hence is an active walker.

year old — for the journal *Computers in Physics* [Lam & Pochy, 1993].

The Hamburg conference was on "Fractals and Disordered Systems" and deserves particular mention. The transparency I presented there (Fig. 3) captures vividly the essence of an active walker. After my talk, David Avnir of The Hebrew University of Jerusalem asked me privately, "How do you get such a novel idea published?" My answer, "I publish it in proceedings," and that was true. At the end, the proceedings editor liked our results [Kayser *et al.*, 1992] so much that he put it on the book cover (Fig. 4). (Avnir was working on structural chirality [Katzenelson *et al.*, 1996] and was impressed by the fact that our AW is able to produce spirals [Freimuth & Lam, 1992].)

In brief, I managed to publish the first three AW papers all in 1992 [Lam *et al.*, 1992; Freimuth & Lam, 1992; Kayser *et al.*, 1992]. More conferences followed.

The conference "Spatio-Temporal Patterns in Nonequilbrium Complex Systems," held in Santa Fe, New Mexico, in April 1993, was very exciting. Almost all the important people in pattern

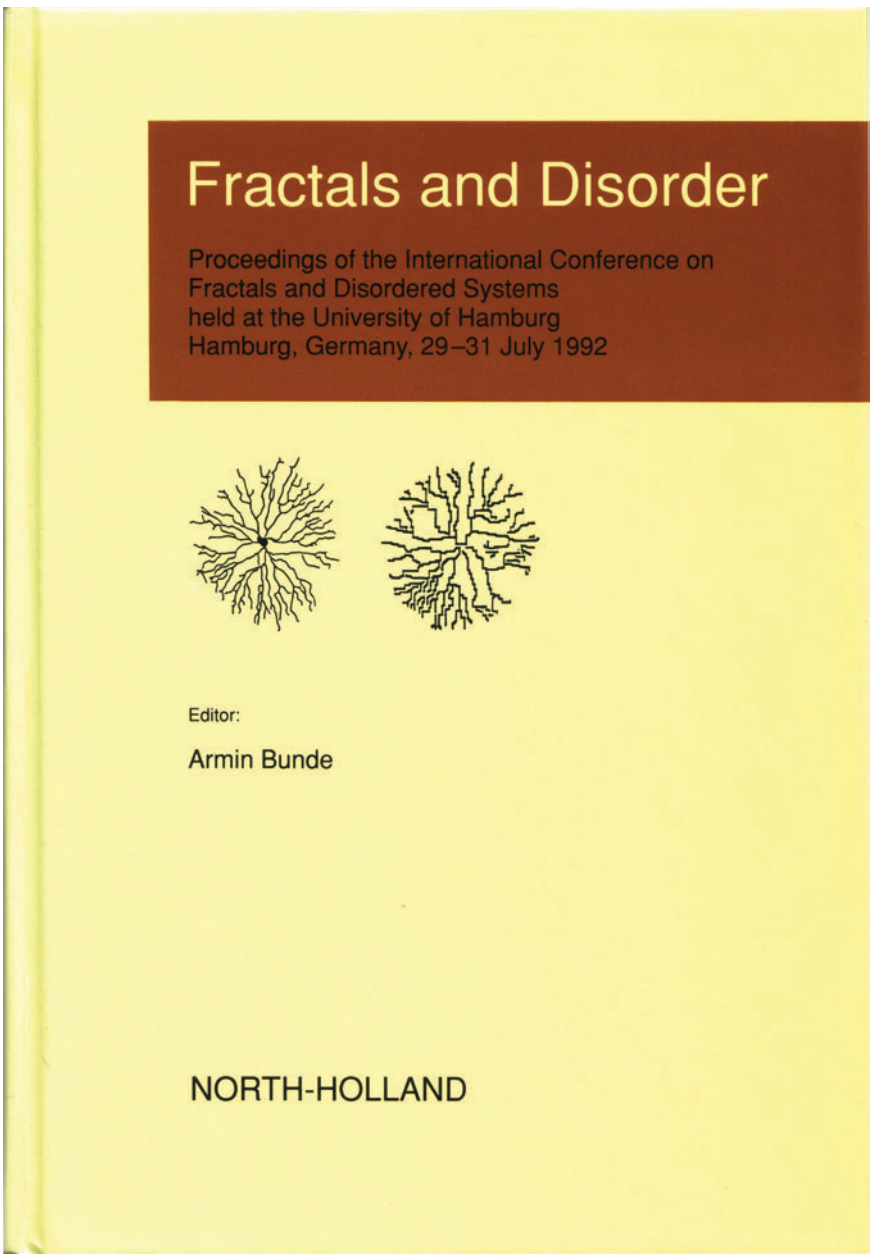

Fig. 4. The book cover of the Hamburg conference proceedings. The two pictures on the cover are reproduced from our article [Kayser *et al.*, 1992] published in the book.

formation were there. I gave the talk "Active Walkers, Landscapes and Complex Systems." It was at this conference that I first met Frank Schweitzer, who presented his work titled "Construction of Path Nets by 'Active' Brownian particles." He knew about my Kitakyushu paper [Lam *et al.*, 1992], and we promised to keep up our contact in the future. That we did. Schweitzer published his first AW paper in 1994, on the clustering of active walkers [Schweitzer & Schimansky-Geier, 1994]. He went on to develop AW further and successfully applied it to many biological and social systems [Schweitzer, 2003].

Since then, AW has been applied by many people worldwide in various simple and complex systems from both the natural and social sciences. Examples include pattern formation in physical, biological and chemical systems such as surface-reaction filaments [Lam *et al.*, 1992; Sheu *et al.*, 1999] and retinal neurons [Kayser *et al.*, 1992], formation of fractal surfaces [Pochy *et al.*, 1993], food foraging of ants [Lam & Pochy, 1993; Schweitzer *et al.*, 1997], worm moving [Lam & Pochy, 1993], bacteria movements and pattern forming [Kessler & Levine, 1993; Ben-Jacob *et al.*, 1994], spontaneous formation of human trails [Helbing *et al.*, 1997], localization–delocalization transitions [Lam, 1995a; Huang *et al.*, 2002], granular matter [Baldassarri *et al.*, 2001], oil recovery [Yuan *et al.*, 1999], economic systems [Lam *et al.*, 1998; Schweitzer, 1998; Savit *et al.*, 1999; Friedman, 2001], and positive-feedback systems [Lam *et al.*, 2002]. More recently, AW has been applied to the study of human history [Lam, 2002].

At the same time, in the last decade or so, agent-based models gained momentum and became a favorite in tackling problems from social systems [Berry *et al.*, 2002]. In these models, a large number of agents are employed; each agent keeps altering an environment and vice versa. These agents are in fact active walkers, and the models are AW models [Epstein & Axtell, 1996; Bonabeau *et al.*, 1999; Schweitzer, 2003].

In the following, the development of AW will be summarized, with more details given to new results (in Secs. 4 and 5). The early review by Lam and Pochy [1993] has since been superseded by [Lam, 1997a]. A popular account of AW appears in [Lam, 2000]. In the present article, while the two major reviews on AW by Lam [1997a] and Scheweitzer [2003] will be frequently referred to, overlaps with them will be kept to a minimum. Also, this present review is extensive but not exhaustive. That would require a book to do it justice.

Finally, a word on nomenclature. In the case of the soliton paradigm, solitons have been given different names such as "walls" and "fluxons" in different applications, and there are different types of solitons such as "kinks" and "breathers" [Lam, 1997b]. With the active walk paradigm, the same thing happened. In fact, due to the flexibility embedded in an AW and according to the applications, the varieties of active walkers are infinite in number. For example, some of these active walkers appear under the name of "Brownian agents" and "bions," and the landscape in a particular AW application is called "sugarscape."

2. The Emergence of Active Walks

The emergence of AW may be viewed from three different perspectives.

2.1. *Active walk as an organizing principle*

The large variety of structures and patterns observed in nature may be classified into a small number of categories; many in the same category resemble each other [Lam, 1998]. To generate them efficiently, it is natural to assume that Mother Nature will adopt a few simple organizing principles. The two extreme cases are the "Principle of Complete Order" and the "Principle of Complete Disorder," leading to, for example, crystals and gases, respectively. A more interesting scheme is the "Principle of Self-Similarity," giving rise to fractals. However, not every structure in Nature is a fractal; there must exist at least one more scheme, and that is the "Principle of Active Walks" [Lam, 1994]. By leaving the landscaping rule and the stepping rule of the walker open (to be specified according to the particular phenomenon under modeling), the AW scheme is very simple and flexible, and hence very powerful. Depending on the rules adopted, AW could give rise to both fractal and non-fractal structures [Lam, 1997a].

2.2. *Active walk as a new kind of walk in modeling*

The movement of a particle — the walker — is called "walks." The use of a walker in modeling physical, biological and even social systems runs a long history. Before 1992, they all practically were *passive* walks. In a passive walk, the

walker does not change anything in its environment. The simplest example is the random walk [Hughes, 1995]. It was first used by Bachelier to describe options in speculative markets [Bachelier, 1900], five years before Einstein applied it in modeling Brownian motion [Einstein, 1905]. In contrast, an *active* walker changes the environment and reacts to the changed environment; AW is obviously a much general and different kind of walk. (Self-avoiding walks and other similarly generalized versions of the random walk leave a marking on the sites visited by the walker. They do not explicitly involve a separate, extended landscape. They are more like passive walks in spirit, even though they could be considered [Lam, 1997a] as extreme cases of AW.)

2.3. *Active walkers as agents used in simulations*

Recently, agent-based simulation is an approach widely used in the modeling of complex systems, especially biological, ecological and social systems [Berry *et al.*, 2002; Epstein & Axtell, 1996; Bonabeau *et al.*, 1999]. The rationale behind this approach is that since complex systems are so complicated, it is usually impossible or impractical to start from differential equations. Instead, the well-honed reduction avenue is followed; to understand an emergent phenomenon one works up from one level below — from the properties of and interactions between the constituents, the agents. In computer modeling, an agent is nothing but a particle with internal states; the particle is usually a point particle, but, in principle, could be a body with spatial dimensions.

The agents may or may not be very smart, but they always have to perform some tasks — such as sensing and measuring the environment, performing some calculations, and changing their locations and internal states. By this definition, the particles employed in Monte Carlo simulations of fluids are also agents; the particles there have to keep track of their own momentum and energy, calculate the conservation laws of momentum and energy, and change directions accordingly — they are very busy agents. In this sense, all simulations (starting from one level down) are agent based.

In an AW, the walker can and has to perform tasks, simple or complicated. For example, before taking the next step in its walk, each walker has to pick up information about its surrounding, and do a calculation according to the stepping rule. They may possess internal states, too. *Active walkers are agents.*

When more than one active walker coexists on a landscape, they interact with each other indirectly through the shared landscape. In reality, interactions between any two physical entities are always indirect in nature. In the microscopic level, two quantum particles interact through the exchange of a messenger. For example, two electrons repel each other by exchanging a photon. Or, in the classical language, one electron first sets up a $1/r$ potential; the second electron "feels" this potential and experiences repulsion. Either way, the interaction is indirect. Macroscopic bodies also interact indirectly. We speak and hear each other through the sound wave in the air medium. People interact indirectly through the Internet (which consists of keyboards, cables, servers, etc.) or reading an advertisement in the newspaper. Instantaneous and direct interactions are only approximations. Ultimately, *all agents are active walkers.*

3. What is an Active Walk?

In an AW, the walker changes the deformable landscape as it walks and is influenced by the deformed landscape in choosing its next step (Fig. 5). The change of the landscape induced by the walker may be short range or long range, may last with a finite lifetime or be permanent; the landscape may have a physical existence or be purely mathematical; it all depends on the phenomenon one wishes to model. The track of the walker forms a filamentary pattern, and the resulting landscape may become a fractal surface.

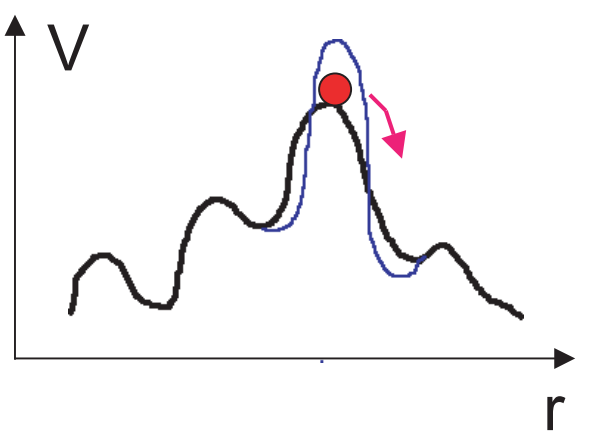

Fig. 5. Sketch of an active walk. The active walker (the red dot) changes part of the landscape potential $V(\boldsymbol{r})$ (from black to blue); the changed potential influences how the walker chooses its next step.

For example, ants are living active walkers [Lam & Pochy, 1993]. When an ant moves, it releases pheromone of a certain type and hence changes the spatial distribution of the pheromone concentration. Its next step is moving towards positions of higher pheromone concentration. In this case, the pheromone distribution is the deformable landscape.

The description of an AW involves two coupled components, viz. the location of the walker $\mathbf{R}(t)$ at time t and the deformable landscape $V(\mathbf{r}, t)$, a scalar potential, where $\mathbf{r}$ is the spatial coordinate. (In other cases, the landscape could be a vector potential, and more than one potential could be used.) The dynamics of an AW are determined by three constituent rules:

(i) The landscaping rule — which specifies how the walker changes the landscape.
(ii) The stepping rule — which tells how the walker chooses its next step.
(iii) The landscape's self-evolving rule — which specifies any change of the landscape due to factors unrelated to the walker, such as diffusion and external influences.

The details of these three constituent rules depend on the system under study. Each of these three rules could be deterministic or stochastic, and might evolve in time according, for example, to genetic algorithms.

Like in the case of random walks [Hughes, 1995], we could have active walks and active flights; either the spatial variable $\mathbf{r}$ or the time variable t, or both, could be discrete or continuous. All these versions are under the umbrella of active walks, though. Again, similar to random walks, the study of active walks could start from the modeling of the walk on a lattice, or from the Langevin equations or the Fokker–Planck equations [Risken, 1989; Gardiner, 1985].

3.1. *The discrete case*

To model AW on a lattice, different landscaping rules and stepping rules have been used [Lam, 1997a]. For example, in the case of a single walker, V at site k could be modified by the active walker with the *landscaping rule*,

$$V(k, n+1) = V(k, n) + W(\mathbf{r}_k - \mathbf{R}(n)) \qquad (1)$$

where $n = 0, 1, 2, \ldots$ is the discrete time (in the unit of t_0); $\mathbf{r}_k$ is the position vector of site k, $\mathbf{R}(n)$ the position of the walker at time n. Different forms of the *landscaping function* W can be assumed. An often used one is $W = W_1$ depicted in Fig. 6. Here, r_2 represents the influence range of the walker; a large W_0 and a small r_1 tend to give close-packed tracks. More generally, the W function could be time dependent, time delayed, or assume a finite lifetime [Lam & Pochy, 1993]. Initially, depending on the system under study, $V(\mathbf{r})$ may be a flat surface, a cone or a slope, or assume some other shape. A nonflat surface will give bias to the walk.

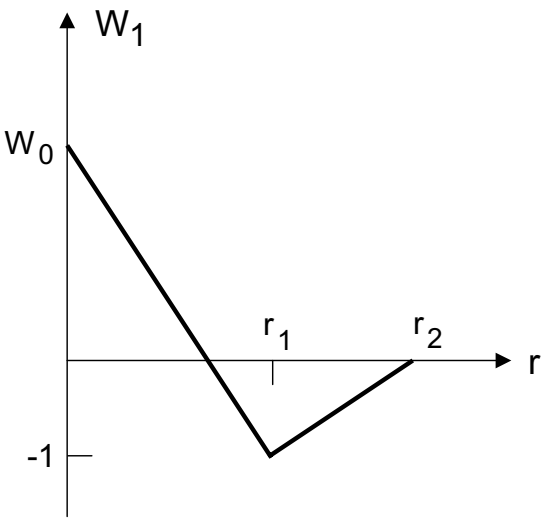

Fig. 6. The W_1 landscaping function.

The stepping rule could be deterministic, probabilistic or fuzzy [Lam *et al.*, 1995]. An example is the "probabilistic active walk" (PAW), defined by the *stepping rule*,

$$P_{ij} \propto [V(i) - V(j)]^{\eta}, \quad \text{if } V(i) > V(j) \qquad (2)$$

and $P_{ij} = 0$, otherwise; the n in V is suppressed. Here P_{ij} is the probability for the walker to step from its present site i to an empty adjacent site j, and η is a parameter. Once the walker moves to its next location, the landscape around it is modified with the same landscaping rule of Eq. (1). And the stepping rule of Eq. (2) is applied again, etc. Note that the walk may terminate if all adjacent sites are higher in V. The first few steps in a PAW using a simple W are shown in Fig. 7.

Branching of the track can be incorporated. If the adjacent vacant position picked happens to have the lowest height in V, then a new walker is put in the site of next lowest in height *provided* its height is within a fraction of that of the first one. The original track branches into two because we now have two walkers (see [Lam, 1997a] for details). The track

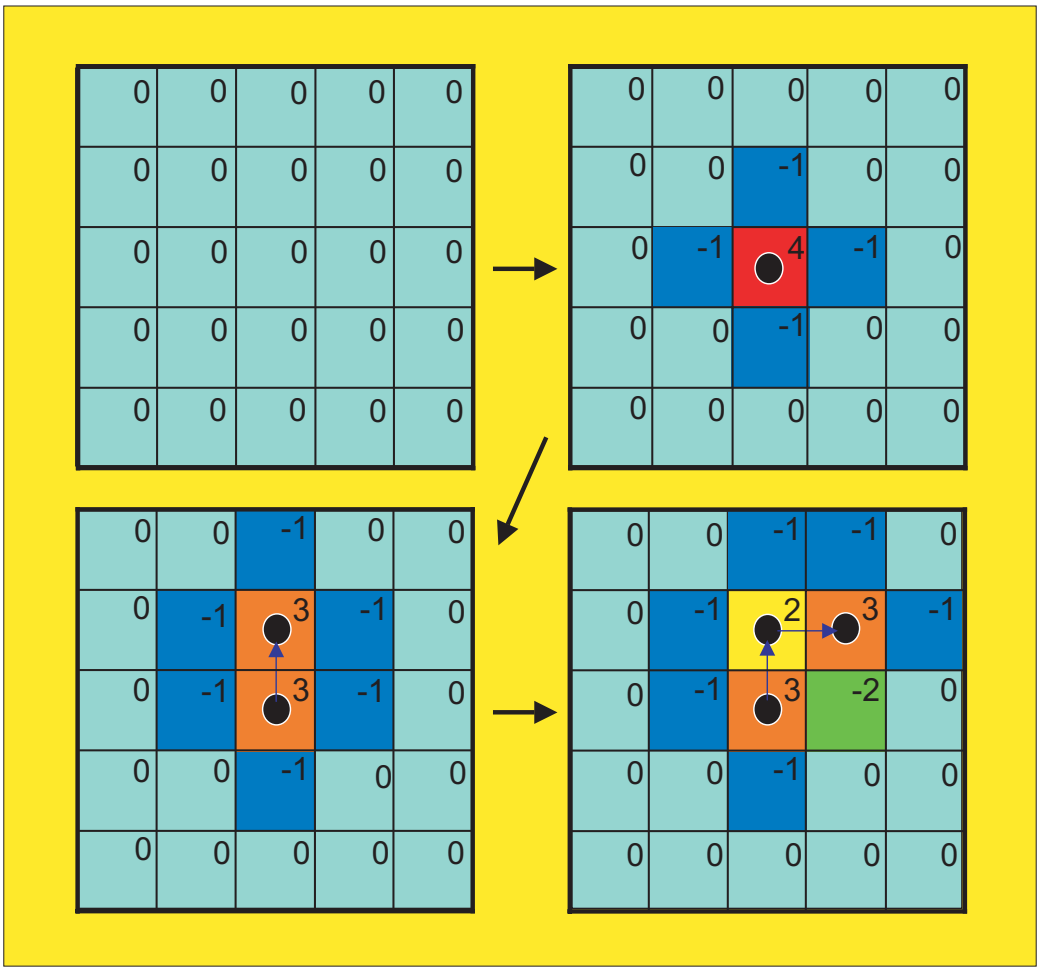

Fig. 7. The first four steps in a PAW model on a square lattice, with a W function such that $V(i) \to V(i) + 4, V(i \pm 1) \to V(i \pm 1) - 1$, and $V(k) \to V(k)$. Here, i is the present location of the walker, $i \pm 1$ the adjacent empty sites, and k are all other sites. The walker's position is represented by a black dot. The landscape is initially flat. The value of V at each site is the number shown in each small box. Time n runs through 0, 1, 2 to 3, indicated by the arrows between the four diagrams. In this probabilistic model, a rerun of the algorithm (corresponding to a different sequence of random numbers implicitly used) may not lead to identical results.

patterns become more interesting in the case of *multiwalkers*. Their movement will influence each other through the shared deformable landscape. Apart from that in Fig. 2, an example is shown in Fig. 8. Good agreement between the AW simulation and patterns from real biological, chemical and physical systems are obtained. (In fact, the dense radial morphology from the PAW shown in Fig. 8 is historically the first one ever generated by any computer model.) It shows that AW is really in the bag of tricks that Mother Nature uses when she wants to produce complicated patterns with minimal effort.

Another kind of stepping rule is that in a "Boltzmann active walk" (BAW), given by

$$P_{ij} \propto \exp\{\beta[V(i) - V(j)]\} \qquad (3)$$

where β plays the role of an inverse temperature. The BAW reduces to a random walk when $\beta = 0$, and a deterministic walk (i.e. the walker always moves to the adjacent site with the lowest height) when $\beta = \infty$. In a BAW, the walker never dies.

Compact patterns can be generated, too — by the PAW, with a lot of branching [Lam, 1995a], or by the "active walk aggregation" (AWA) model [Lam & Pochy, 1993]. In the AWA, one starts with a single particle. The landscape around this particle is changed by a landscaping rule; one of the perimeter sites of the aggregate is chosen with a probabilistic rule; then a new particle is added to this chosen site. The process is repeated.

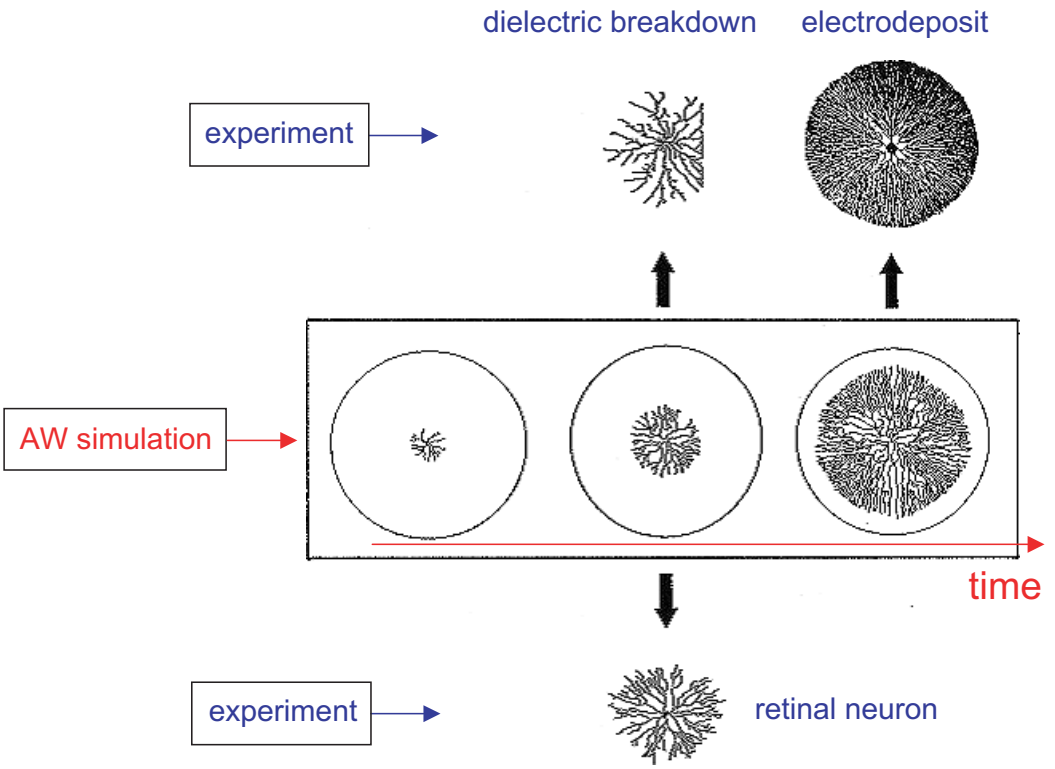

Fig. 8. Comparison of active walk simulations with experimental data. (Middle) Patterns enclosed in the rectangle, from left to right, represent the time development of a pattern generated by the PAW model with a W_1 function [Lam *et al.*, 1992]. Four walkers are initially placed at the center, close to each other; branching is allowed. The initial landscape is a cone pointed upward, introduced to give an outward motion to the walkers. The arrows outside of the rectangle point toward the experimental patterns, with which the corresponding computer patterns should be compared. (Top left) Chemical reaction pattern induced by dielectric breakdown in a thin layer of oil [Pan *et al.*, 1995]. (Top right) A dense radial morphology from electrodeposit in a $ZnSO_4$ cell [Sawada *et al.*, 1986]. (Bottom) A retinal neuron, redrawn from Fig. 1.0, credited to Masland, R. H., in *Fractals and Disordered Systems*, eds. Bunde, A. & Havlin, S. (Springer, NY, 1991).

3.2. *The continuous case*

The continuous case is obtained in the continuum limit of the discrete model, in which the spatial and time variables become continuous. The corresponding stochastic equations, either the Langevin or the Fokker–Planck equations, need to be *derived* according to the particular model adopted. Or, one may simply start with a pair of coupled partial differential equations involving $\mathbf{R}(t)$ and $V(\mathbf{r}, t)$. For example, the Langevin equations for a *single* active walker could be given by

$$m\frac{\mathrm{d}^2\mathbf{R}}{\mathrm{d}t^2} = -\mu\frac{\mathrm{d}\mathbf{R}}{\mathrm{d}t} - \int \mathrm{d}\mathbf{r}\delta(\mathbf{r}-\mathbf{R})\nabla V(\mathbf{r},t) + \mathbf{F}(t) \tag{4}$$

and

$$\frac{\partial V(\mathbf{r},t)}{\partial t} = D\nabla^2 V(\mathbf{r},t) + t_0^{-1}W(\mathbf{r}-\mathbf{R}(t)) \tag{5}$$

where m, the mass of the walker, represents the inertial effect; μ is a damping coefficient; t_0 is relaxation time constant; $\mathbf{F}$ is a fluctuating force; D is a diffusion constant; W, the landscaping function, represents how the walker changes the landscape. This pair of equations is not easy to solve. The generalization of Eqs. (4) and (5) to the case of multiwalkers is straightforward. The $\mathbf{R}$ in Eq. (4) becomes $\mathbf{R}_i$, with i indexing the ith active walker; and the $\mathbf{R}$ in Eq. (5) is now replaced by $\sum_i \mathbf{R}_i$.

The Fokker–Planck equations

$$\frac{\partial p(\mathbf{r},t)}{\partial t} = \frac{\partial}{\partial \mathbf{r}}[p(\mathbf{r},t)\nabla V(\mathbf{r},t)] + D_w\nabla^2 p(\mathbf{r},t) \tag{6}$$

and

$$\frac{\partial V(\mathbf{r},t)}{\partial t} = D\nabla^2 V(\mathbf{r},t) + t_0^{-1}\int \mathrm{d}\mathbf{r}' W(\mathbf{r}-\mathbf{r}')p(\mathbf{r}',t) \tag{7}$$

are not necessarily simpler, where $p(\mathbf{r}, t)$ and D_w are the probability density and the diffusion constant of the walker, respectively.

These two sets of stochastic equations are relatively new in the stochastic literature. For example, in the standard textbook on Fokker–Planck equations [Risken, 1989], only the case of a particle moving in a *fixed* potential is discussed — not the case of a coupled, deformable potential discussed here. Solvable AW models are hard to come by. In Sec. 4, a simple but solvable stochastic AW model will be presented.

3.3. *Landscapes in active walks*

The landscape in an AW could be physical or abstract in its origin. Examples of physical landscapes include the pheromone distribution due to ants, the sand surface for a darkling beetle, the paths of percolation in soft materials, chemical distribution in chemotaxis of bacteria, and nutrition distribution for fish.

On the other hand, abstract landscapes are mathematical artifacts. For example, urban growth can be modeled by the aggregation of active walkers. Initially, a "value" (or *fitness*) can be assigned to every piece of vacant land, according to its location. For example, a lot on the flatland will have a higher value than one located on the hills; a river nearby can increase the value of the lot, etc. The value could be taken to be the probability that the lot will be developed, by having a house or factory built on it. Once this happens, the value of the lands nearby will be increased and a new house may be added nearby or somewhere. The process is repeated. In this scheme, the house acts like an active walker in the AWA model. Such a model is more realistic and flexible than the correlated percolation model used by Makse *et al.* [1995].

Another example is the fitness landscape employed in evolution biology [Kauffman, 1993]. Every species is in coevolution with other species. The presence of species A affects the fitness landscape of species B, say, which in turn changes the fitness landscape of A; the changed landscape of A then determines how A will move. Now, if this evolution process is described by a simple model involving A alone (with B hidden behind the scene), it would look like that A deforms its own landscape at every step of its movement; i.e. A acts like an active walker [Lam *et al.*, 1998]. The third example concerns the phenomenon of increasing returns in economics, in which the landscape is the fitness of two competing products [Lam *et al.*, 1998].

In some cases, the landscapes, though physical, could be hidden from the eye; they may be overlooked and the problem becomes insolvable. An example happened in the filamentary growth in electrodeposits. In the electrodeposit growth in a thin cell of two parallel electrodes, filaments like the trees in a forest are generated [Lam *et al.*, 1990]. These tree-like filaments are perpendicular to the electrodes and are well separated from each other; the separation depends on the electrode voltage, solution concentration, and cell thickness. What enables the filaments to "know" the existence of their neighbors and adjust accordingly their separation from each other has remained a puzzle for a couple of years. It turns out that the convection of the solution, the medium the filaments embedded in, is crucial. The growth of a filament can be represented by an AW; the solution is the hidden landscape that the walkers share. It is this hidden landscape that enables the electrodeposit trees to communicate with each other [Lam, 1995b].

4. A Solvable Case: The Two-Site Active Walk Model

The simplest AW model is the two-site model, proposed by Lam *et al.* [1998] and subsequently developed in [Lam *et al.*, 2002]. This model can be used to describe positive- or negative-feedback systems, such as the competition of two consumer products in the market.

4.1. *The a-walk*

In the two-site model, a single active walker (a-walker) jumps between two sites or stays at the same site at every time step. The landscape is represented by the potential V, called fitness, with values $V_1(n)$ and $V_2(n)$ at the two sites respectively, where n is the discrete time. At time n the a-walker picks site k ($k = 1, 2$) with probability P_k, which is proportional to some given function $f(V_k)$. Once a site is picked, its fitness will be modified by

$$V_k(n+1) = V_k(n) + a_k \tag{8}$$

The process is then repeated. (See Fig. 9.) The probability P_1 that site 1 will be picked is equal to $1/[1 + f(V_2)/f(V_1)]$. Obviously, $P_1 + P_2 = 1$. The active walk in this model is a Markovian process.

A monotonic increasing function f represents a positive-feedback process; a monotonic decreasing

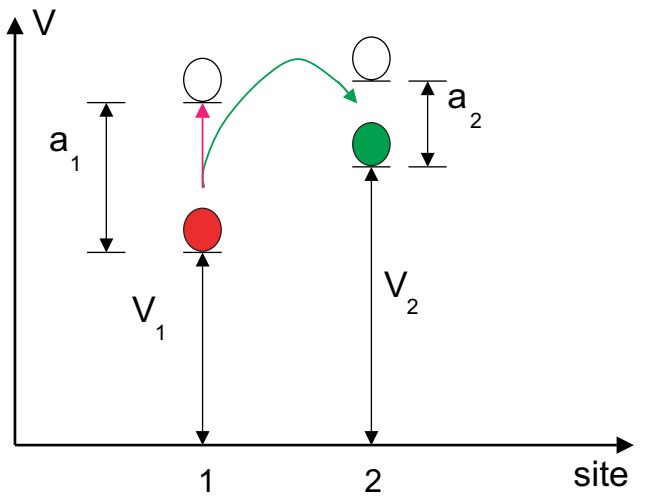

Fig. 9. Sketch of the a-walk in the two-site active walk model. The active walker (the red dot) may choose to stay at site 1; V at site 1 then rise by a height a_1. If the walker jumps to site 2, V at site 2 will be increased by a_2.

f, a negative feedback. A one-bump f function corresponds to a positive feedback followed by a negative feedback. A saturated function such as $f(V_k) = \tanh V_k$ could mimic the saturation effect experienced by a consumer when a good thing is taken too many times.

4.2. *The p-walk*

For the case where $f(V_2)/f(V_1)$ depends only on s ($\equiv V_1 - V_2$), we have $P_1 = q(s)$ for some function q which is related to the function f. Under this condition, the a-walk can be mapped to a walk on the s axis. In addition, if r ($\equiv a_2/a_1$) is rational, the model is reduced to a one-dimensional "position-dependent probabilistic walk" (called p-walk) with a single probabilistic walker (p-walker) moving on the infinite s axis. Let $a \equiv a_1$ and $s(n)$ be the p-walker's position on the s axis at time n. Site 1 being picked by the a-walker at time n [so $V_1(n+1) = V_1(n) + a$ and $V_2(n+1) = V_2(n)$] corresponds to

$$s(n+1) = s(n) + a \tag{9}$$

and the p-walker takes one step of size a to the right on the s axis. Both the a-walker and the p-walker make these moves with the same probability $q(s)$. Similarly, if site 2 is picked, we have $V_2(n+1) = V_2(n) + ra$ and thus

$$s(n+1) = s(n) - ra \tag{10}$$

and the p-walker jumps to the left with probability $1-q(s)$. (See Fig. 10.) Note that while the a-walker

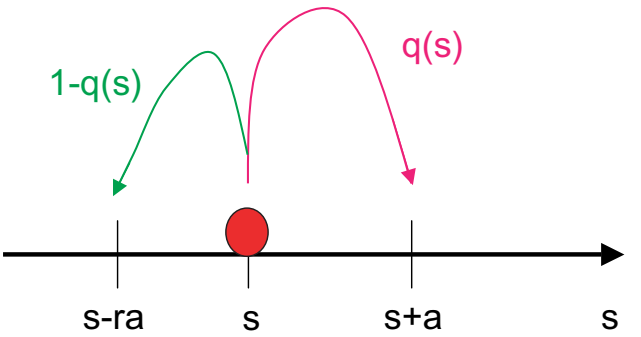

Fig. 10. Sketch of the p-walk in the "position-dependent probabilistic walk", which is equivalent to the a-walk under suitable conditions (see text). The probability for the walker (the red dot) to jump to the right (to the position $s + a$) is given by $q(s)$; to the left (to position $s - ra$), by $1 - q(s)$.

can stay at the same site or jump to the other site, the p-walker must jump either left or right.

In the master equation description, the probability $p(s, n+1)$ of the p-walker being at position s at time $n+1$ is given by

$$p(s,n+1) = q(s-a)p(s-a,n) + [1-q(s+ra)]p(s+ra,n) \tag{11}$$

subject to the initial condition of $p(s,0) = 1$ if $s = s_0$, and $p(s,0) = 0$, otherwise.

In the rest of Sec. 4 we assume

$$f(V_k) = \exp(\beta V_k) \tag{12}$$

where β is the inverse "temperature". The corresponding q function is given by

$$q(s) = [1 + \exp(-\beta s)]^{-1} \tag{13}$$

Note that the model reduces to a random walk when $\beta = 0$, and a deterministic walk (a walk without reverse in direction) when $\beta = \infty$.

4.3. *Numerical results*

Equation (11) is solved numerically by iteration. Typical result is plotted in Fig. 11. Soon after the beginning, a peak appears near s_0; it then splits into two peaks, moving away from each other. At large time, these two peaks move without change in shape and velocity, like two *solitons*. These solitons can be understood from the Fokker–Planck equation governing the p-walk [Lam, 2003]. For $s_0 > 0$ and $r \leq 1$, the area of the right-peak (in the $s > 0$ region) $A_R(n)$ is larger than $A_L(n)$, the area of the left peak (in the $s < 0$ region). The two peaks are mirror-symmetrical in shape with respect to the

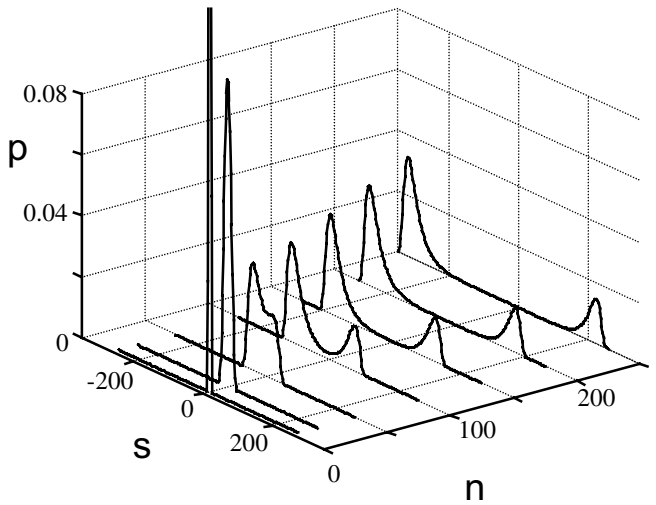

Fig. 11. Numerical solution of $p(s,n)$ from Eq. (11). Here $a = 1,\ s_0 = 2,\ \beta = 0.08$ and $r = 1.4$.

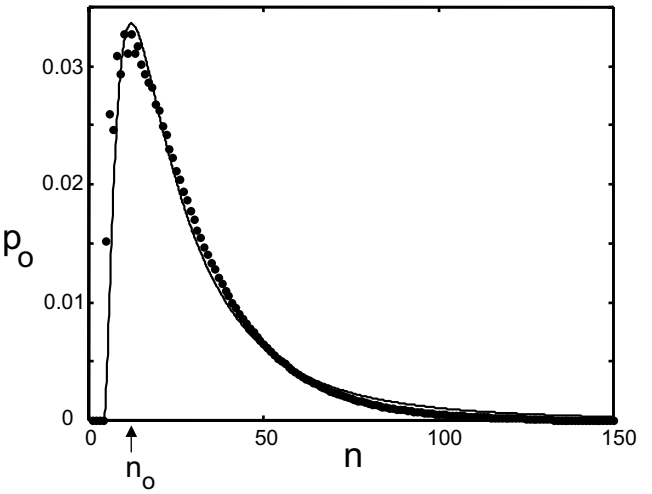

Fig. 12. Dependence of p_0 on n. Solid dots are numerical results, with $a = 1, r = 1, s_0 = 5$ and $\beta = 0.1$. The solid line is drawn to guide the eye, which peaks at $n = n_0$.

vertical s axis, and hence $A_R(n) = A_L(n)$, if and only if $s_0 = 0$ and $r = 1$.

The result could be understood easily in terms of two products competing with each other. In such a case, the fitness of a product V_k may be taken to be the sale of k, the number of product k sold. The right peak area $A_R(n)$ represents the probability that product 1 will dominate over product 2 at time n. The case of $s_0 = 0$ and $r = 1$ corresponds to the two products being equal in all aspects, so they have equal chance of winning. The case of $r > 1$ (meaning product 2 is better than product 1) in Fig. 11 corresponds to product 2 (the latecomer if $s_0 > 0$) having a larger chance of winning the market, because the left-peak area is larger.

The probability that product 2 will catch up with product 1 at time n is given by $p_0(n) \equiv p(0,n)$. Figure 12 shows a typical numerical result for $p_0(n)$, which is equal to zero for $n < s_0$. A nonzero p_0 implies that the latecomer can actually catch up; the maximum chance of catching up occurs at $n = n_0$. Consequently, the latecomer should not give up trying before time n_0.

4.4. *Analytical results*

The analytical results presented in this section are only for the case of $r = 1$. Let $i \equiv s/a$, $i_0 \equiv s_0/a$ and $b \equiv \beta a$. The master equation (11) becomes

$$p(i,n+1) = q(i-1)p(i-1,n) + [1 - q(i+1)]p(i+1,n) \qquad (14)$$

4.4.1. *Right peak area and left peak area*

The right peak area A_R is constant at large time, and depends on the three parameters i_0, b and r only. The area of the left peak A_L is given by $A_L = 1 - A_R$. The numerical result for A_R with $r = 1$ is plotted in Fig. 13. The curves can be fitted nicely by

$$A_R(n; i_0, b) = \frac{1}{2}\mathrm{erfc}\left[-i_0\left\{\frac{2n}{\exp(-bn) + bn}\right\}^{-\frac{1}{2}}\right] \qquad (15)$$

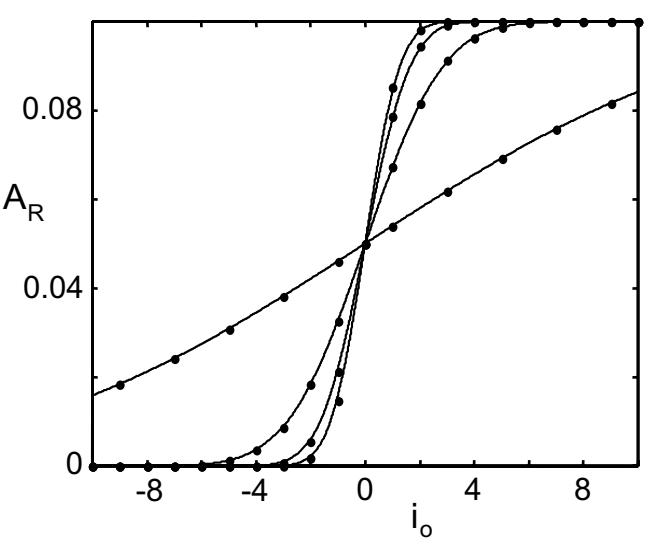

Fig. 13. Dependence of A_R on i_0 and b. Here $n = 100$ and $r = 1$. In the $i_0 > 0$ region, the curves from bottom to top correspond to $b = 0, 0.2, 0.6$ and 1, respectively. Solid dots are numerical results; curves are analytical results from Eq. (15). Excellent agreement between the two is achieved.

for n large (so that the left and right peaks are well separated from each other). Let us look at two limiting cases.

(a) $\underline{b = 0}$

For $b = 0$, the p-walk reduces to the random walk. Equation (15) becomes

$$A_R(n; i_0) = \frac{1}{2}\text{erfc}[-i_0(2n)^{\frac{1}{2}}] \tag{16}$$

which is the exact result expected for a random walk.

(b) $\underline{n \to \infty}$

For $n \to \infty$, Eq. (15) becomes

$$A_R(\infty) = \frac{1}{2}\text{erfc}\left[-i_0\left(\frac{b}{2}\right)^{\frac{1}{2}}\right] \tag{17}$$

which in fact is an exact result (see Sec. 4.4.2).

4.4.2. *Right-exit probability and left-exit probability*

Given i, i_R and i_L with $i_L \leq i \leq i_R$, let $R(i)$ be the right-exist probability that the p-walker at initial position i will eventually reach position i_R, with the absorption boundary condition (i.e. if the p-walker ever reaches i_L before it reaches i_R, the walk is terminated). For a p-walker starting at position i ($\neq i_R$ or i_L) to right-exit, it may move right first and then right-exit, or move left first and then right-exit. Therefore, we have

$$R(i) = q(i)R(i+1) + [1 - q(i)]R(i-1), \quad i_L < i < i_R \tag{18}$$

subject to the boundary condition of $R(i_R) = 1$ (right-exit) and $R(i_L) = 0$ (absorption).

For the special case of Eq. (13), the solution of Eq. (18) is given by

$$R(i) = \frac{\sum_{j=i_L}^{i-1} \exp\left[-b\left(\frac{j+j^2}{2}\right)\right]}{\sum_{j=i_L}^{i_R-1} \exp\left[-b\left(\frac{j+j^2}{2}\right)\right]} \tag{19}$$

which can be proved by induction on i. Replacing the summation by an integral as an approximation, the limit of $R(i)$ as $i_L \to -\infty$ and $i_R \to \infty$ is found to be

$$R_\infty(i) \approx \frac{1}{2}\text{erfc}\left[-i\left(\frac{b}{2}\right)^{\frac{1}{2}}\right] \tag{20}$$

Replacing i by i_0, Eq. (20) becomes Eq. (17), as expected.

The left-exit probability $L(i)$ is defined as the probability that the p-walker, starting from position i, will eventually reach i_L, with i_R being the absorbing boundary. It is given by

$$L(i) = 1 - R(i) \tag{21}$$

4.4.3. *Average displacement of the p-walker*

The average displacement of the p-walker is defined by

$$\langle i(n)\rangle \equiv \sum_{i=-\infty}^{\infty} ip(i, n) \tag{22}$$

By Eqs. (14) and (22) we have

$$\langle i(n+1)\rangle = \langle i(n)\rangle + \sum_{i=-\infty}^{\infty} [2q(i) - 1]p(i, n) \tag{23}$$

For $i_0 = 0$, we have $\langle i(n)\rangle = 0$ for all n. In the following, the case of $i_0 \neq 0$ is considered. Without loss of generality, we also assume that $i_0 > 0$.

Again, for the special case of Eq. (13) and in the continuum limit, Eq. (23) can be solved analytically in the two regimes that $|bi| \ll 1$ and $|bi| \gg 1$. The analytical results for these two limiting cases are obtained with variables x and t, where x is i in the continuum limit and t, that of n.

(a) $\underline{|bx| \gg 1}$

With the details omitted here, we obtain the equation

$$\frac{\text{d}\langle x(t)\rangle}{\text{d}t} = [2R_\infty(x_0) - 1]\tanh\left(\frac{b\langle x(t)\rangle}{2}\right) \tag{24}$$

and the corresponding solution

$$\langle x(t)\rangle = \frac{2}{b}\text{arcsinh}\left\{\exp\left[\left(\frac{b}{2}\right) \times (t|2R_\infty(x_0) - 1| + c)\right]\right\} \tag{25}$$

The constant of integration c is determined by requiring $\langle x(t)\rangle$ from Eq. (25) to coincide with that from the simulation curve at $t = t_{\text{m}}$. The simulation

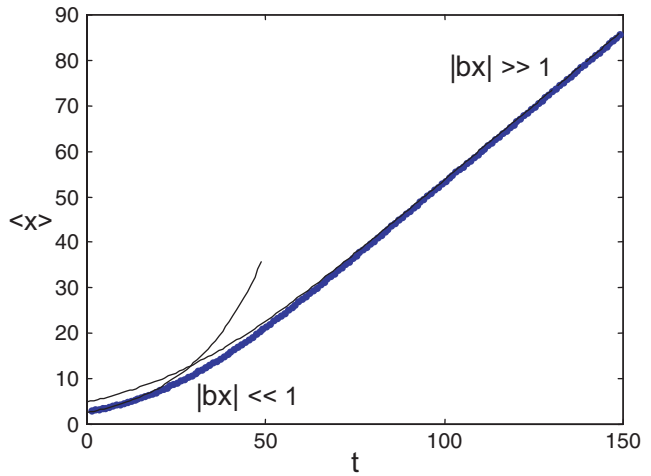

Fig. 14. Dependence of the average displacement of the p-walker $\langle x(t)\rangle$ on time t. Here $x_0 = 3, b = 0.1$ and $r = 1$. Analytical results in the two limiting regimes (the two solid curves) from Eq. (25) for t large, and Eq. (28) for t small, agree very well with the numerical result (blue curve). (The deviations of the solid curves from the blue one are where the analytical results are not supposed to be valid; they are kept here to guide the eye.)

curve $\langle x(t)\rangle_{\text{run}}$ is obtained by simulating the p-walk many times and averaged over the runs. Thus,

$$c = \frac{2}{b}\ln\left[\sinh\left(\frac{1}{2}b\langle x(t_{\text{m}})\rangle_{\text{run}}\right)\right] - t_{\text{m}}|2R_\infty(x_0) - 1| \tag{26}$$

In practice, t_{m} is chosen to be the maximum t in the simulation curve, since our $\langle x(t)\rangle$ (and hence $b\langle x(t)\rangle$) from Eq. (25) is a large $|bx|$ approximation and is not expected to fit well for small t.

(b) $|bx| \ll 1$

The equation for this case is given by

$$\frac{\mathrm{d}\langle x(t)\rangle}{\mathrm{d}t} = \left(\frac{b}{2}\right)\langle x(t)\rangle \tag{27}$$

which has the solution

$$\langle x(t)\rangle = x_0 \exp\left(\frac{bt}{2}\right) \tag{28}$$

where x_0 is x at $t = 0$. From Fig. 14, we can see that the analytical results from Eqs. (25) and (28) agree very well with the numerical data.

5. Surface-Reaction Filamentary Patterns: Experiments and Active Walk Models

As shown in Sec. 1, historically, surface-reaction filamentary pattern played an important role in the birth of active walks. Here, a general discussion of pattern formation will be presented, followed by experiments and AW modeling for surface-reaction filamentary patterns in Hele–Shaw cells. The cells thickness may be uniform or nonuniform (in wedged cells). The results in the wedged cell case are new. The thermal threshold AW models, also new, are pretty general and should be applicable in other cases of pattern formation.

5.1. *Pattern formation in general*

One can hardly fail to notice the striking similarity between the ramified patterns formed by rivers, trees, leaf veins and lightning. These branching patterns are different from compact patterns observed in snowflakes, clouds and algae colonies. How does nature generate these patterns? Is there a simple principle or universal mechanism behind these pattern-forming phenomena? Progress has been made in answering these profound questions in the last two decades [Lam, 1998; Cross & Hohenberg, 1993; Ball, 1999].

Patterns existing in nature and laboratories may be classified into two types [Lam, 1998]: (A) those involving an interface, and (B) those that do not. Type A patterns can be further separated into two classes, viz. (A1) filamentary, or (A2) compact. (See Fig. 15.) Of course, when filamentary patterns are much magnified, they appear as compact. The distinction between A1 and A2 depends on the scale used in the observation, but the classification is beneficial in model building.

Examples of A1 patterns are surface-reaction filaments induced by dielectric breakdowns [Lam *et al.*, 1991] and cracks [Mardar & Fineberg, 1996]. A2 patterns include viscous fingers, dendrites in crystal growth and directional solidifications, bubbles and flame propagation [Saffman, 1990; Pelce, 1988; Pelce *et al.*, 2004]. B type patterns appear, for example, in Rayleigh–Bérnard convection [Cross & Hohenberg, 1993] and the electroconvection of liquid crystals [Ribotta, 1992; Buka & Kramer, 1996]. (See Fig. 16.) Here, the case of surface-reaction filaments (discovered in our own lab), the prototype of filamentary growth patterns, will be discussed in some detail.

5.2. *Experiments in uniform cells*

A Hele–Shaw cell (i.e. two parallel glass plates separated by thin insulating spacers, with cell thickness

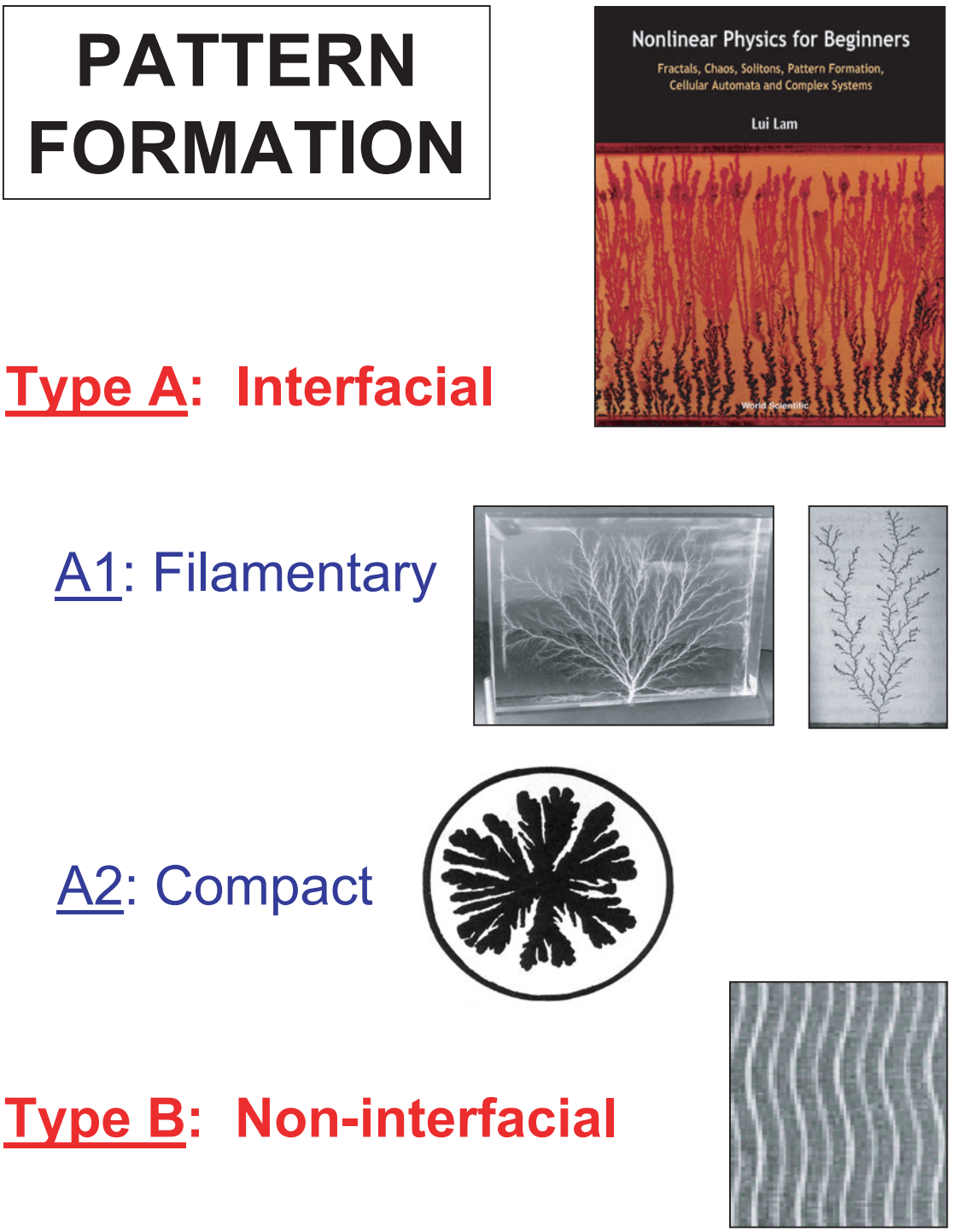

Fig. 15. Classification of patterns. Examples of type A (consisting of A1 and A2) and type B are taken from the book [Lam, 1998]. The picture on the book cover, shown on the upper right corner, depicts the multiple morphological transitions in a linear cell of electrodeposits, discovered by Lam's Nonlinear Physics Group.

6–25 μm) consists of two glass plates coated with transparent, conducting indium tin oxide (ITO) in the inner surfaces. A DC or AC voltage is applied across the cell, creating a uniform electric field perpendicular to the plates. The cell is filled with oil or other liquids, such as liquid crystals. (See Fig. 17.) The voltage V is either (i) increased gradually above a threshold V_c and then maintained at constant, or (ii) turned on abruptly from zero to a value above V_c and kept constant. In either case, a flash of light is

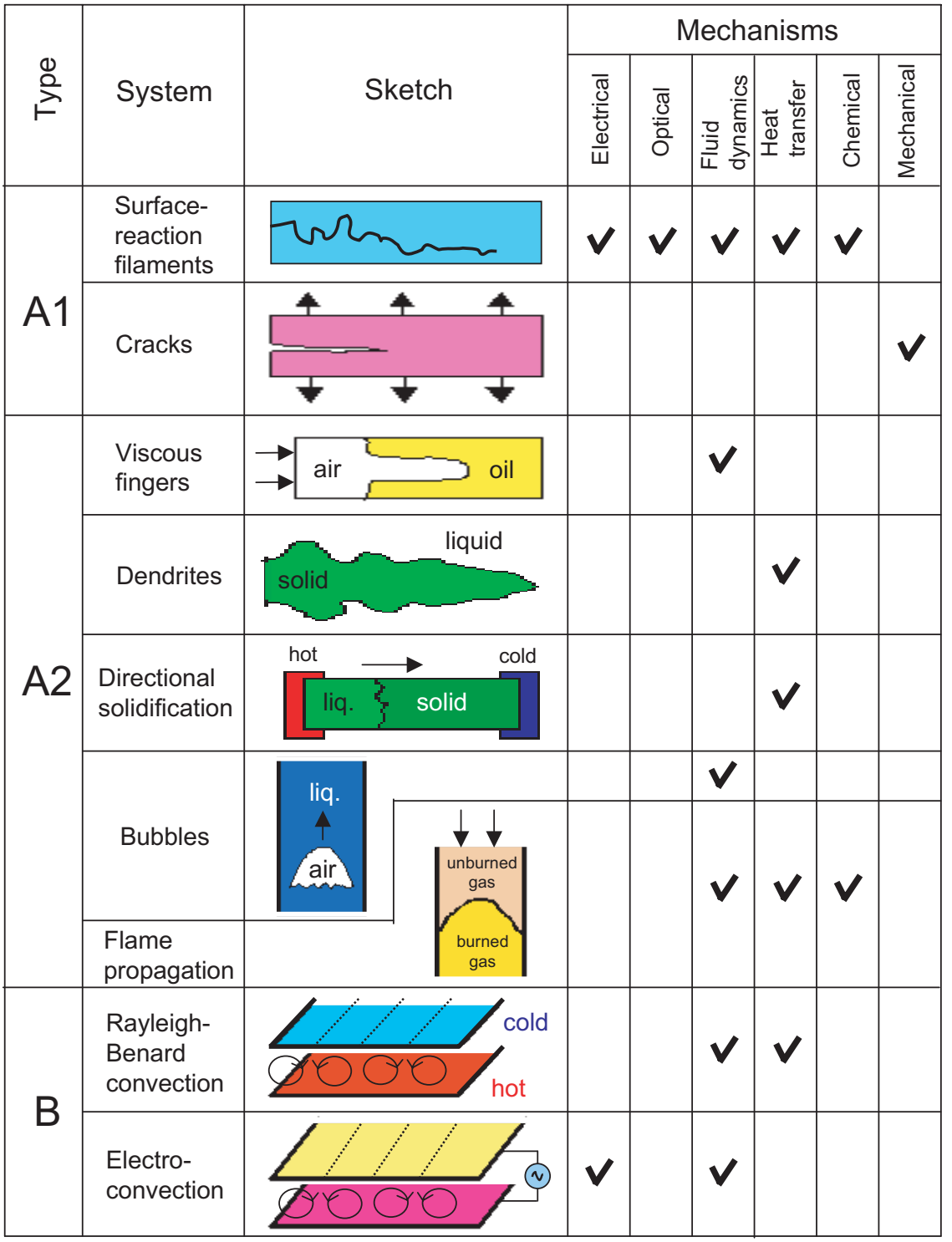

Fig. 16. Different types of patterns and their mechanisms.

observed and a filamentary pattern is left behind when viewed from outside the plates. When the cell is opened the filaments are found to consist of black powders. In fact, the same pattern is "etched" onto the inner surfaces, with the width of the filaments on the positive-potential plate larger than that left on the negative-potential plate [Lam *et al.*, 1991].

Such an experiment was first done in our laboratory [Lam *et al.*, 1991; Lam *et al.*, 1992; Kayser *et al.*, 1992] and subsequently elsewhere [Pan *et al.*, 1995; Sheu *et al.*, 1999; Sheu *et al.*, 2000]. Some

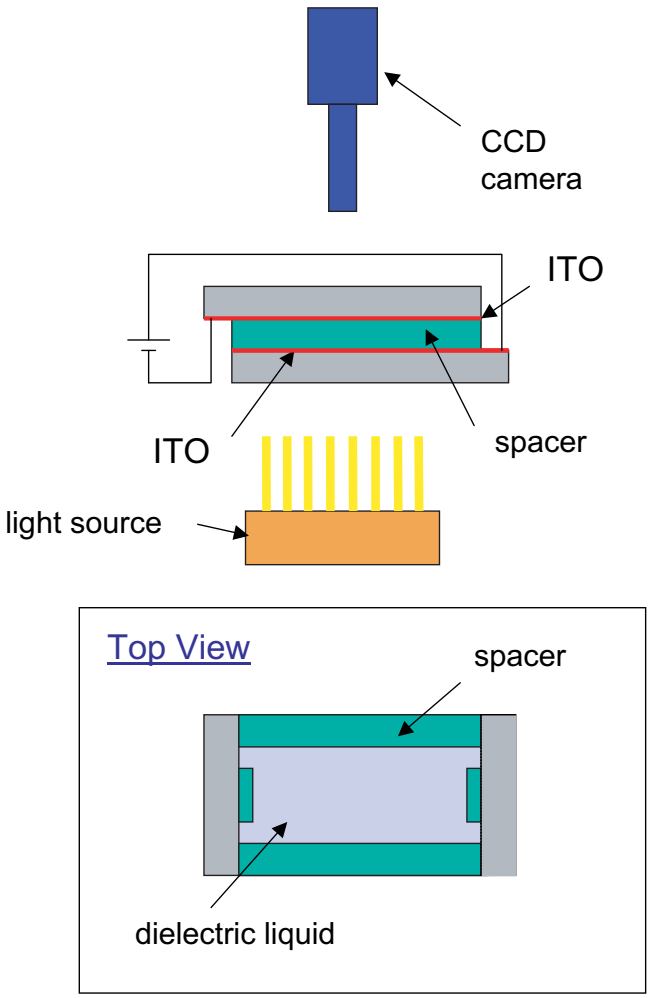

Fig. 17. Sketch of the setup for a uniform cell in surface-reaction experiments.

typical patterns are shown in Fig. 18. Essentially, each filament in the pattern undergoes three stages: birth, growth and death (Fig. 19). The birth stage exists in three different forms:

(i) A ring is formed first, and several filaments branch out from the ring (Fig. 20).
(ii) Several filaments start from a point.
(iii) A single filament starts from a point.

There are also three types of growth:

(i) Dense winding — slow growth, with growth velocity $v \ll 1\,\mathrm{m/s}$, smooth filament, no branching (Fig. 21).
(ii) Radial wiggling — fast growth, $v \sim 1\,\mathrm{m/s}$, wiggling filament, with branching (Fig. 22).
(iii) Random moving — very fast growth, $v \gg 1\,\mathrm{m/s}$, smooth filament intermitted with wiggling segments, with no or rare branching (Fig. 23).

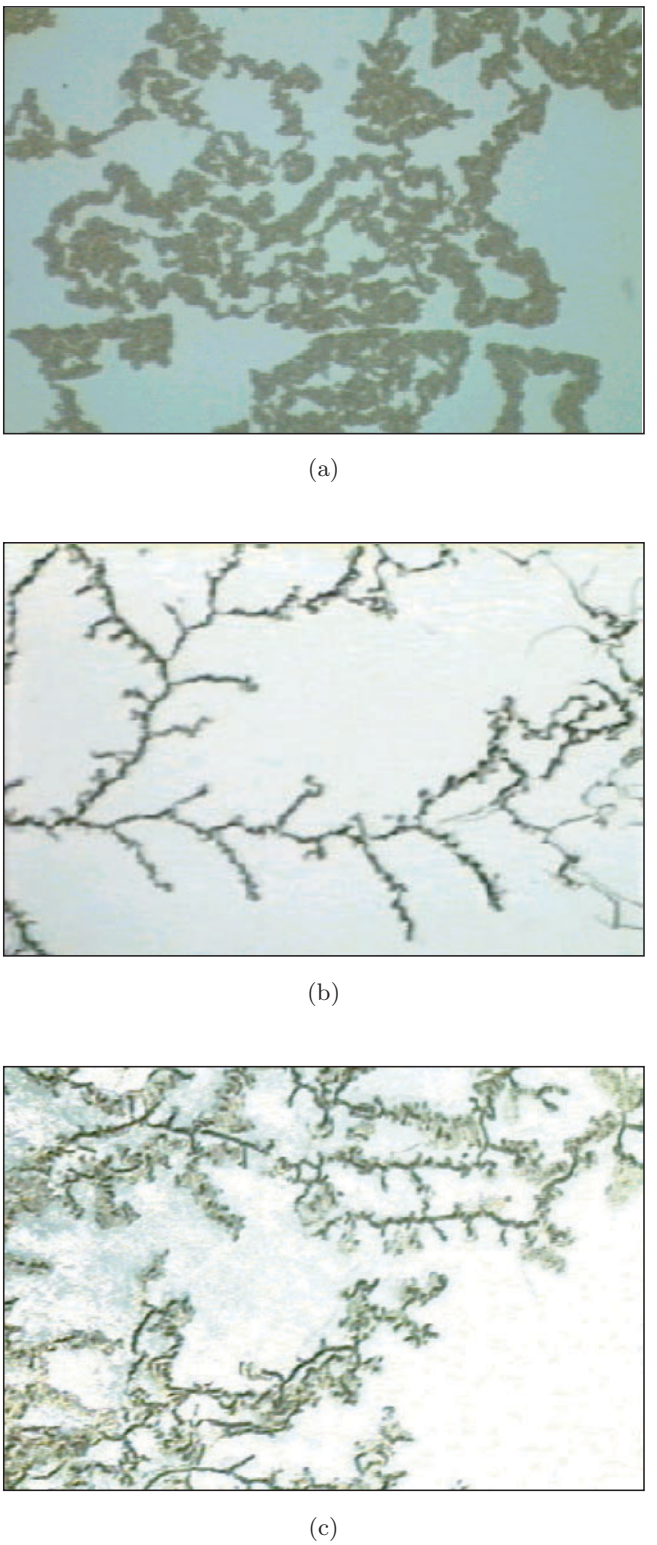

(a)

(b)

(c)

Fig. 18. Some experimental surface-reaction filamentary patterns. (a) Air cell; (b) oil cell; (c) liquid crystal cell.

Death also occurs in three forms (Fig. 24):

(i) Blunt — the filament stops with a thick end in empty space.

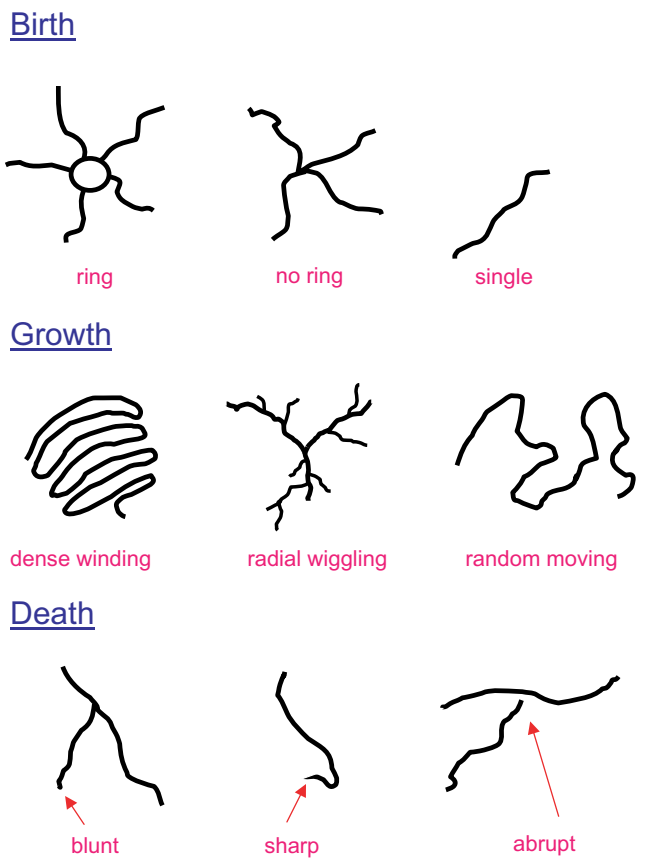

Fig. 19. Sketch of the birth, growth and death of a filament. Each of the three stages exists in three possible forms.

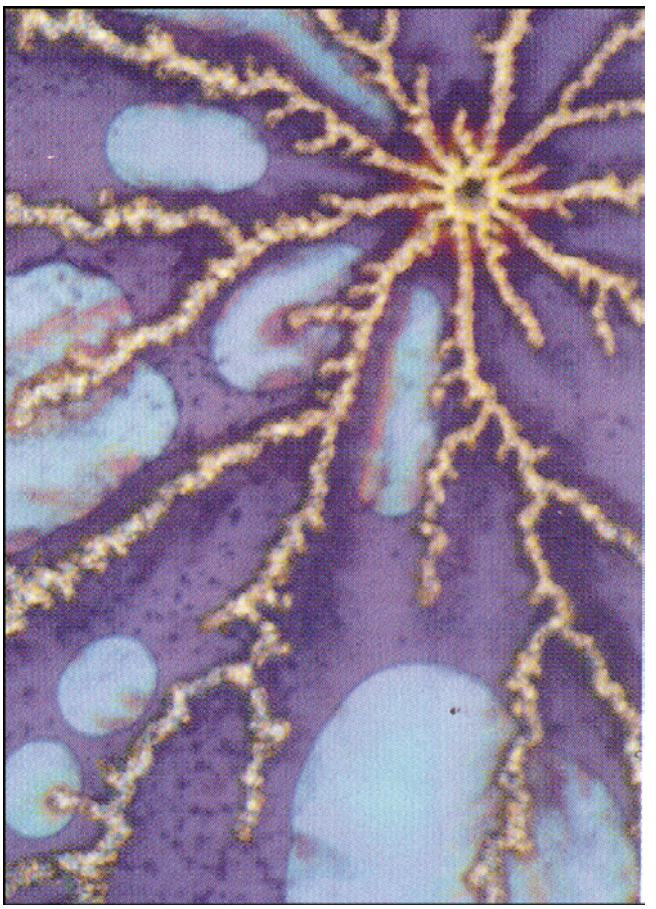

Fig. 20. Birth of filaments starting from a ring observed in experiments [Pan *et al.*, 1995].

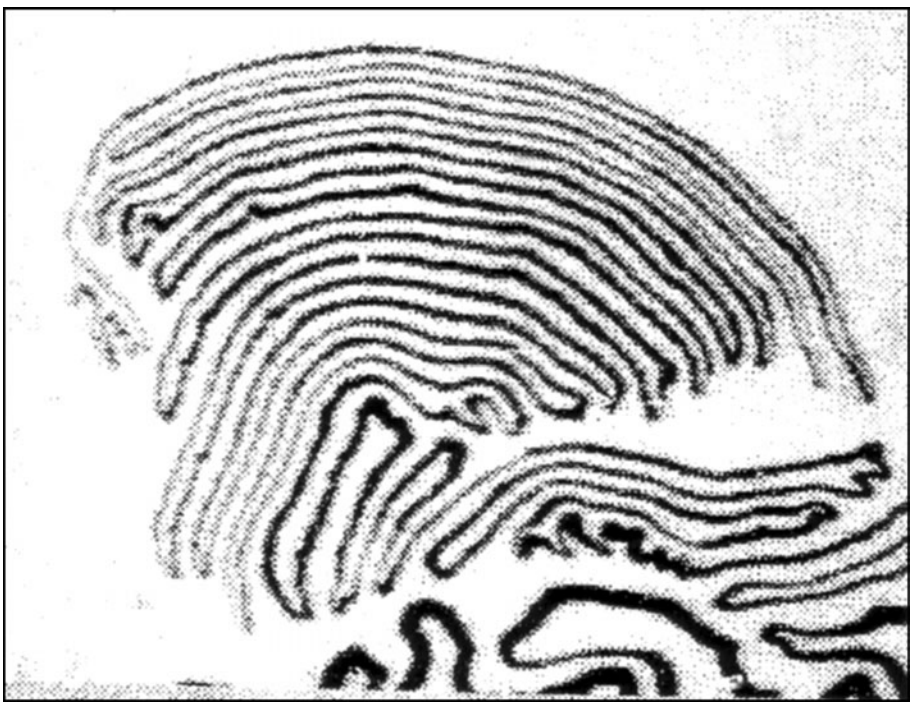

Fig. 21. "Dense winding" of a filament observed in experiments.

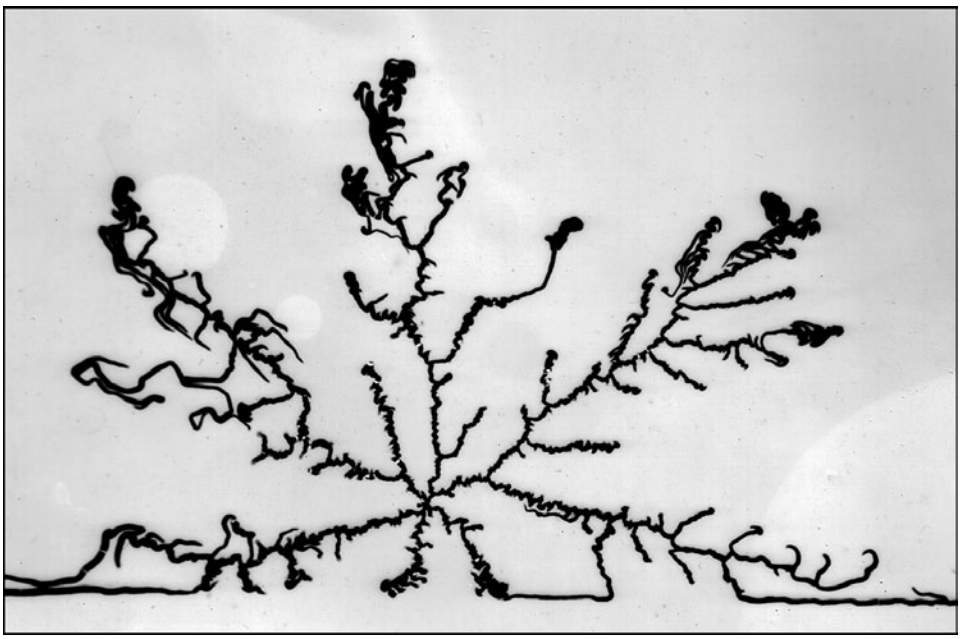

Fig. 22. "Radial wiggling" occurs near starting point observed in experiments. Some dense winding sets in at later time, a spontaneous morphological transition. The bottom horizontal line is due to the cell edge. (Courtesy of Ru-Pin Pan.)

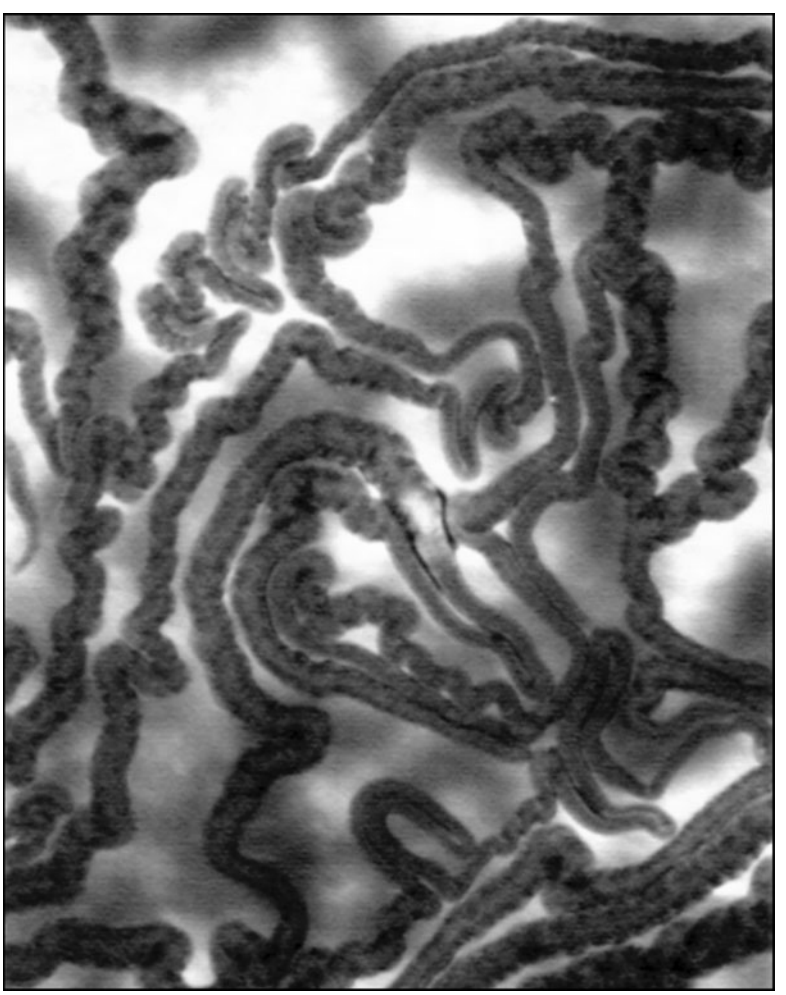

Fig. 23. "Random moving" of filaments observed in experiments.

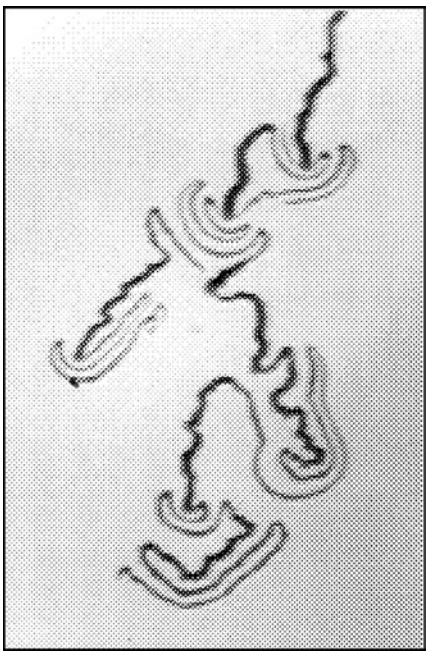

Fig. 24. Death of filaments observed in experiments.

(ii) Sharp — the filament stops with a sharp end in empty space.
(iii) Abrupt — the filament ends just before hitting another filament.

Incidentally, in an isolated occasion when a very high voltage was mistakenly applied to a uniform liquid crystal cell, a single large circular bubble was observed at the end of the process, as shown in Fig. 25. This confirms that gas is released during the filament formation.

As pointed out above, in a uniform cell, the starting points of the filaments cannot be controlled. To overcome this problem, and to find out more about these filaments, wedged cells are used.

5.3. *Experiments in wedged cells*

Two kinds of wedged cells are used, viz. linear wedged cells or radial wedged cells.

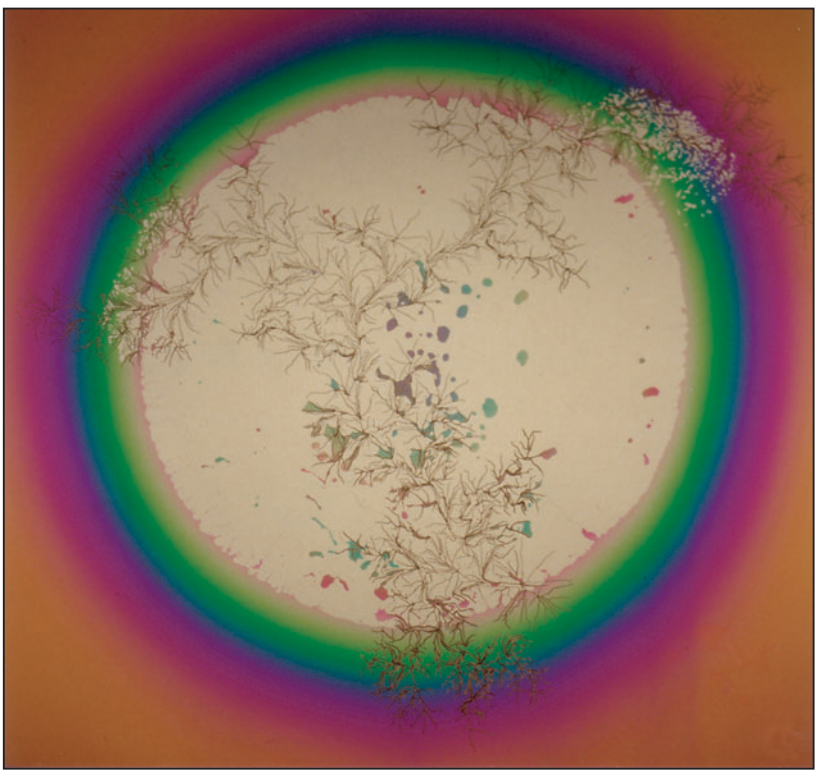

(a)

Fig. 25. Experimental surface-reaction filamentary pattern observed in a nematic liquid crystal cell under a very high voltage. A large circular bubble shows up bright under parallel polarizers (sandwiching the cell) in (a), and dark under crossed polarizers in (b), indicating that the bubble indeed consists of isotropic gas, and not liquid crystals. The few bright spots within the dark area in (b) are due to the presence of leftover liquid crystal droplets. The diameter of the bubble is 4.4 cm. (Picture (a) appears in the book cover of [Lam, 1997a].)

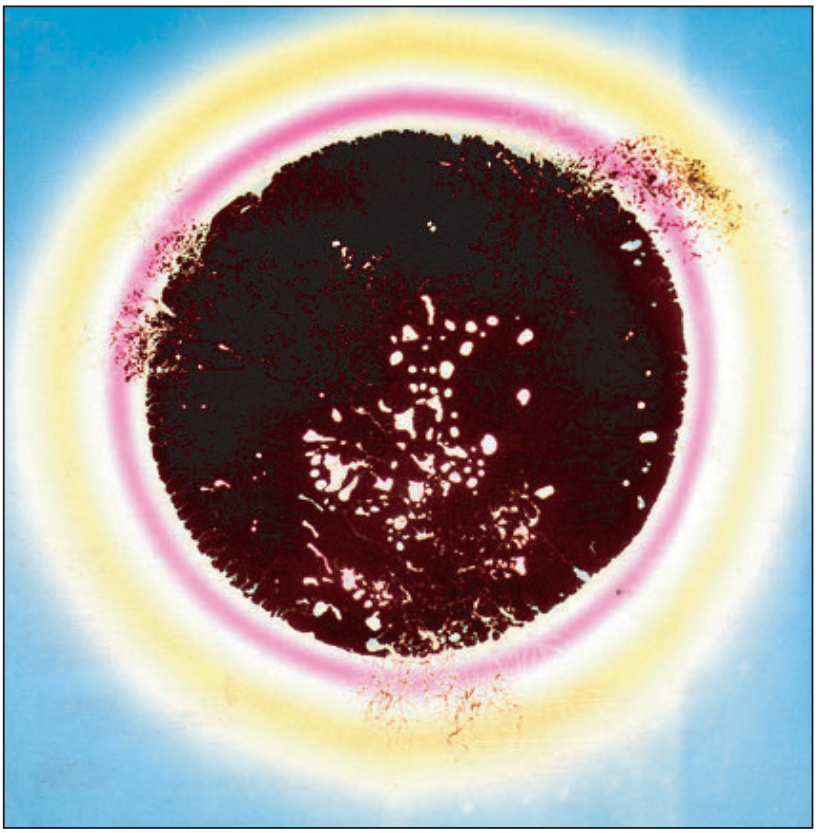

(b)

Fig. 25. (*Continued*)

5.3.1. *Linear wedged cells*

The setup for a linear wedged cell is sketched in Fig. 26. The cell is filled with air and is open to air along the two long sides. The DC voltage is increased from zero and then maintained at 35 V. A sodium lamp is used as the light source. Pattern growth at the constant voltage stage is presented in Fig. 27. The filaments grow from the left edge of the cell where the electric field is highest, as expected. New filaments keep on appearing as time increases. The electroluminescence accompanying the dielectric breakdown [Zaky & Hawley, 1973] of air is indeed observed as bright spots at the growth tip of each filament. Some filaments branch, others do not (Fig. 28). The filaments do cross each other (Fig. 29) and this is due to the fact that air is the cell medium used — so that even though tracks are formed on the inner surfaces of the plates due to chemical reactions, no substantial solid chemical products are left behind between the cell plates to block the advance of a late-coming filament, in contrast to what is observed in an oil cell (see Sec. 5.2). In other words, the tracks in an

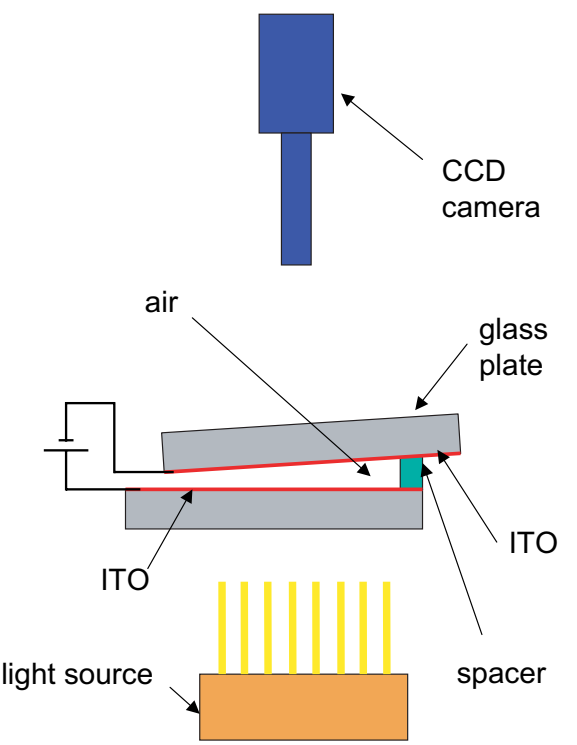

Fig. 26. Sketch of the setup of a linear wedged cell in surface-reaction experiments.

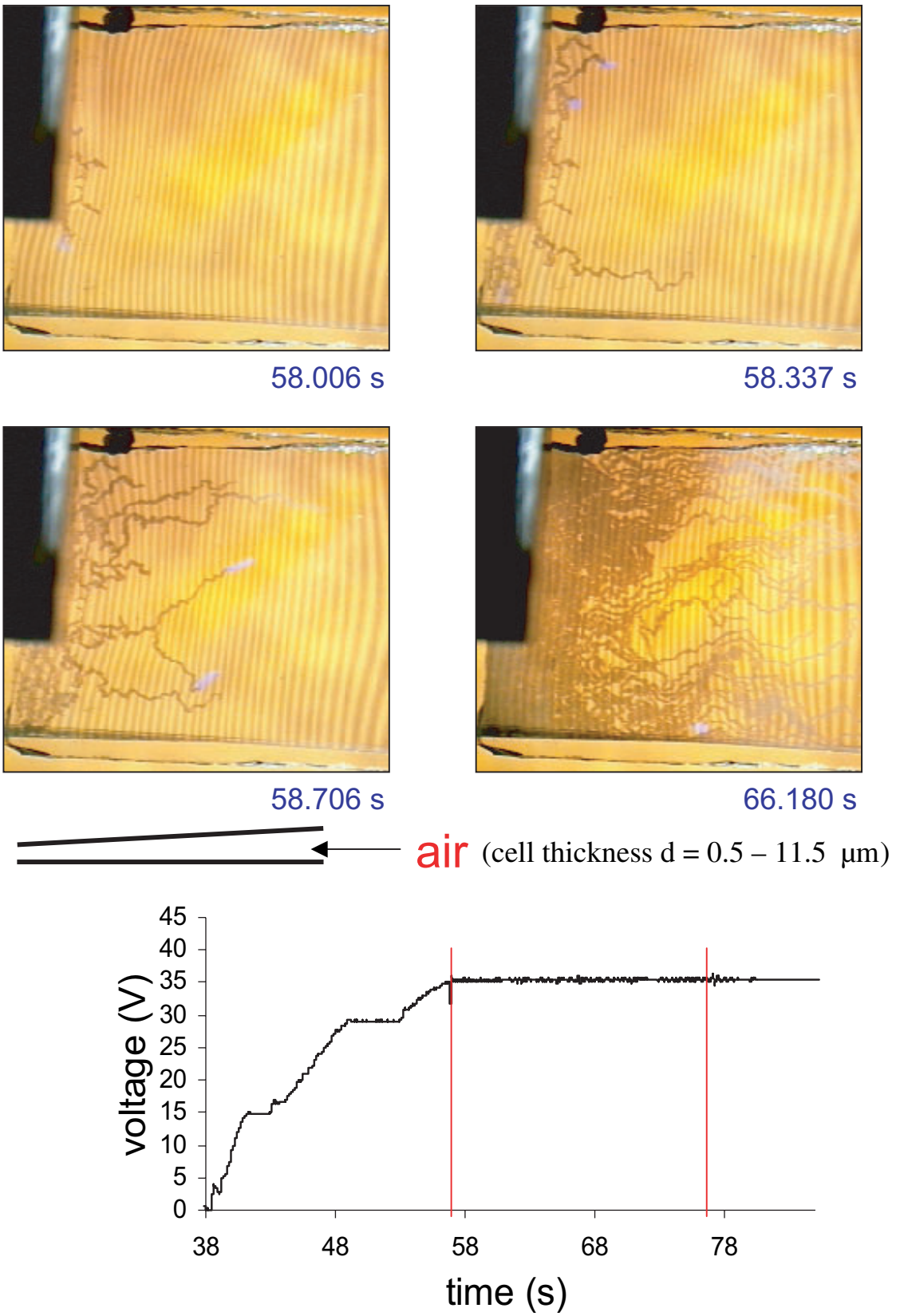

Fig. 27. Experimental surface-reaction filaments in a linear wedged cell filled with air. The use of sodium light in illumination gives rise to the yellow color and the interference stripes, which allow an accurate determination of the cell thickness locally. (More details are given in Figs. 28–30.)

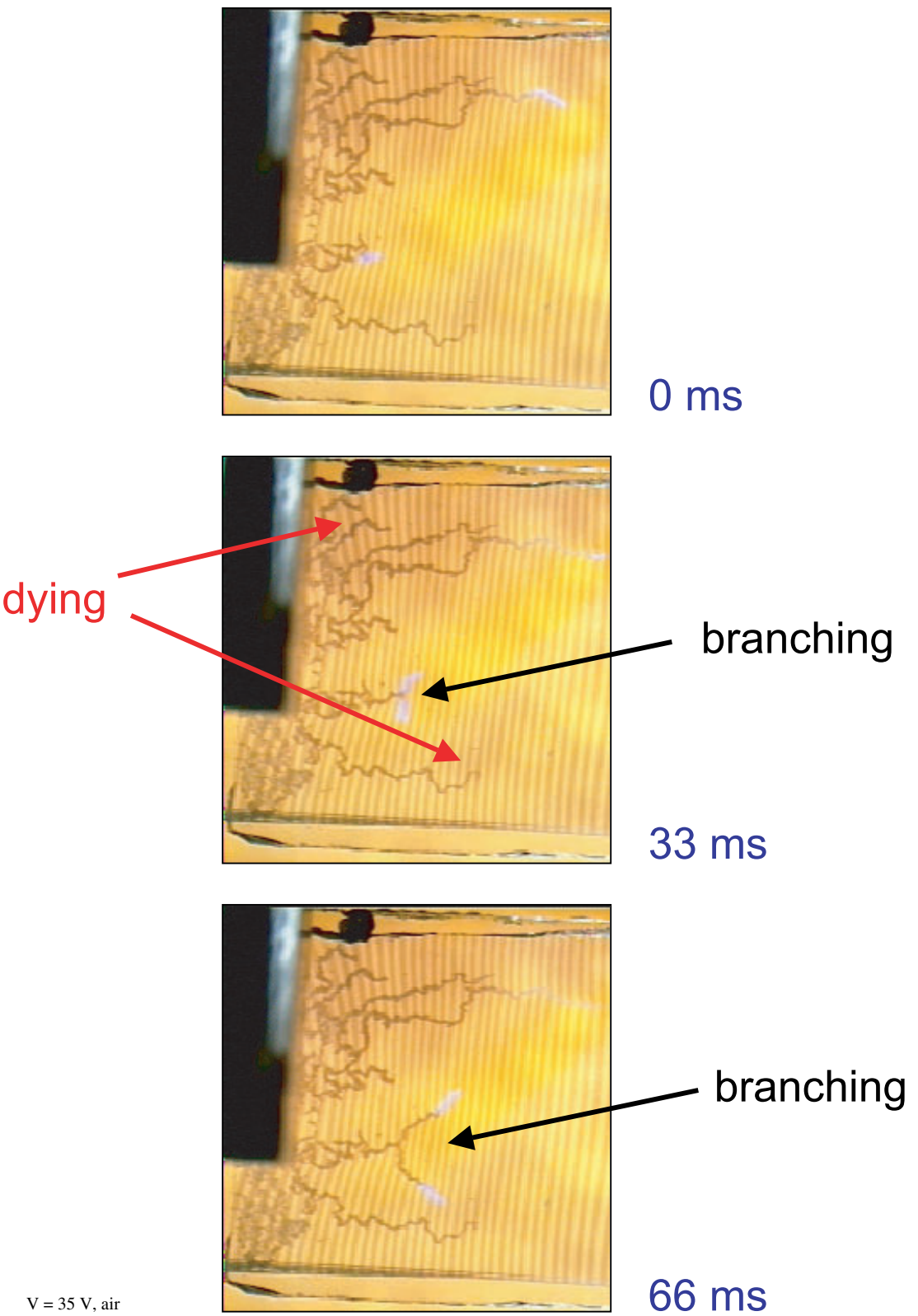

Fig. 28. Experimental results from a linear wedged air cell, showing the electroluminescence light (in white color) at the growth tip, and the branching and dying of surface-reaction filaments.

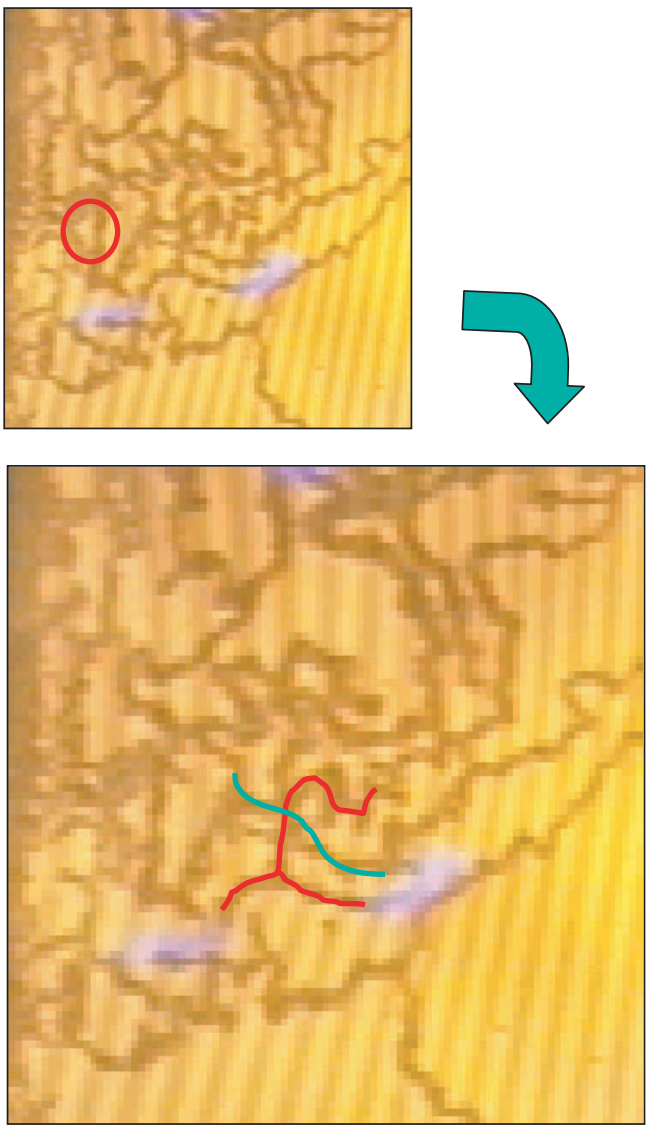

Fig. 29. Crossing of two filaments (indicated by the green and red lines in lower picture) observed in a linear wedged air cell. The lower picture is the blow up of the area indicated by the red circle in the upper picture.

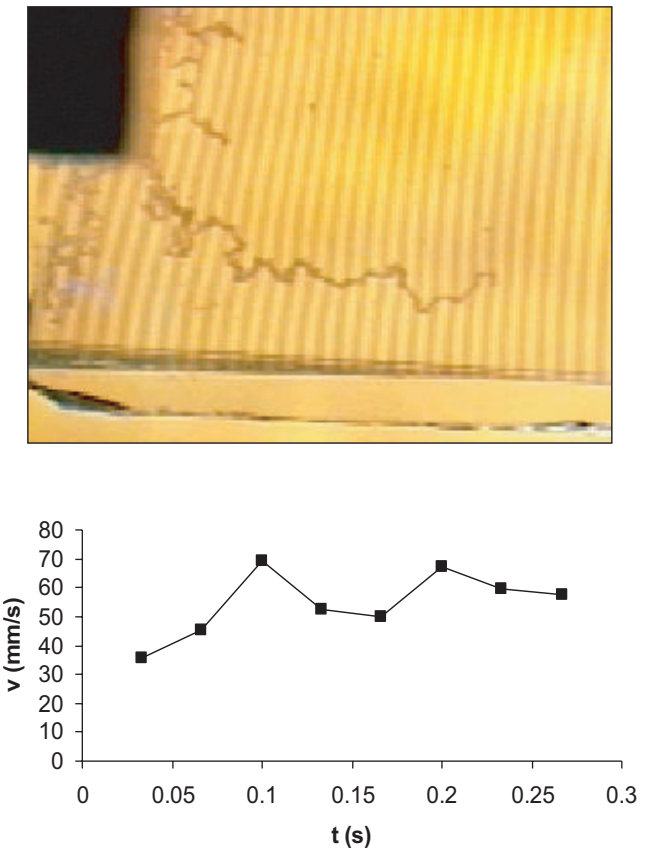

Fig. 30. The growth velocity of a single filament as a function of time observed in a linear wedged air cell.

air cell could be self-crossing while those in an oil cell are truly self-avoiding. The growth speed of a single filament is plotted in Fig. 30. The speed is about 6 cm/s, slower than that in the uniform cells.

In short, with a linear wedged *air* cell we succeed in

(i) controlling the birthplace of the filaments,
(ii) slowing down their growth rate (so that a camcorder can be used to capture the dynamics),
(iii) observing the creation and movement of a bright spot at the tip of the growing filament,
(iv) confirming the absence of blocking chemicals deposited in between the plates (in contrast to the oil cell case).

5.3.2. *Radial wedged cells*

In a radial wedged cell filled with mineral oil, the thickness of the cell is the smallest at the center. A radial wiggling pattern, with branching, is observed to start from a location very near the center (Fig. 31). Some filaments change to dense winding as they grow further away from the center, similar to the case in a uniform cell (Fig. 22). However, due to technical limitations we are not able to control the cell thickness and the starting point precise enough in these cells. Yet, we are able to capture unambiguously the formation of bubbles and the electroluminescence growth light in such an oil cell (Fig. 32). The bubble in Fig. 31 appears as viscous fingers, similar to those observed in a radial Hele–Shaw cell where oil is displaced by air, or in electrodeposits in an open circular dish [Lam *et al.*, 1990; Lam, 1995b].

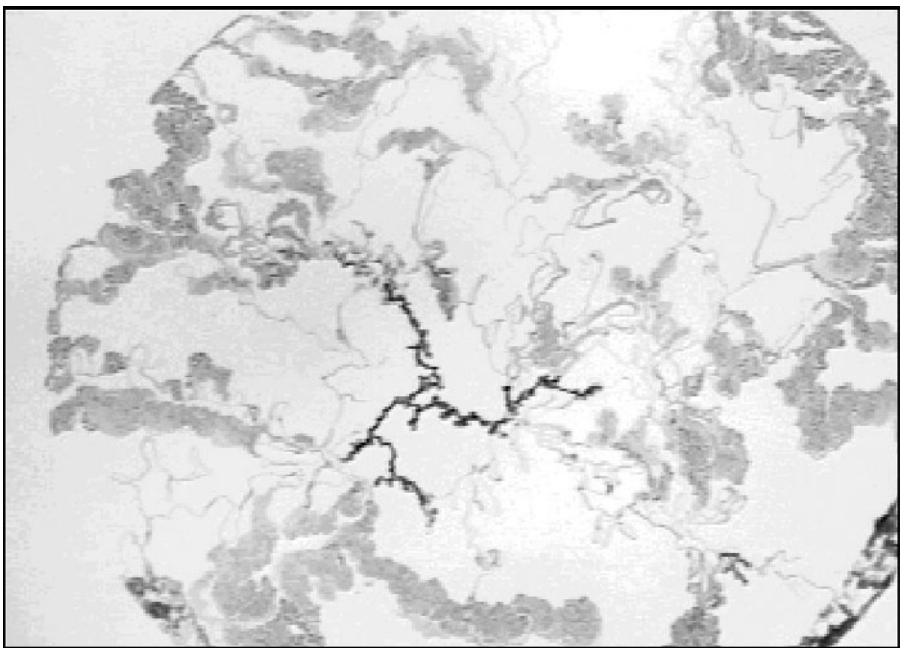

Fig. 31. Morphological transition from radial wiggling to dense winding observed in a radial wedged oil cell.

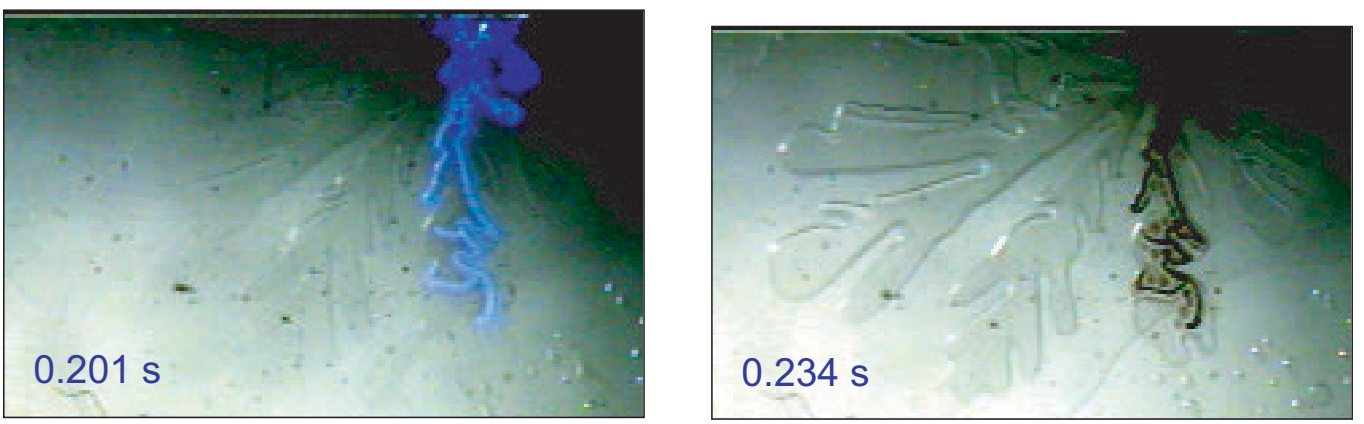

(a) (b)

Fig. 32. Observation of gas bubble (in the form of viscous fingers), and electroluminescence light during the growth of a filament. This light occurs at the filament's growth tip. The light shows up as a continuous blue line in (a), because each picture here has an exposure time of 1/30 s and is thus effectively a multiple-exposure picture. The blue line represents the shape of the filament. After growth, the blue light is gone and the material that made up the filament is black in color, as shown in (b).

5.4. *Active walk modeling*

The formation mechanism of these surface-reaction filaments involves physical and chemical processes, and is very complicated. Roughly speaking, it goes like this. With a high enough voltage, dielectric breakdown (DB) of the molecules inside the cell happened suddenly at a point where the voltage is locally the highest. (In a "uniform" cell, this starting point is due to irregularity of the ITO coating or the plate surface itself which is impossible to control; in a linear wedged cell, at the short edge with the smaller thickness.) More DB is induced by collision and occurs along the path perpendicular to the cell plates at this point. The resulting ions and electrons rush towards the plates in opposite directions. Heat is generated. Chemical reactions between the IPO and the cell fluid happen, giving rise to more heat and leaving behind black powders

in the space between the plates at this point. However, if everything actually occurred along a vertical path, we should see a dark spot — i.e. no horizontal filaments breaking the cylindrical symmetry of the cell. Somehow, some of the ions and electrons may not move vertically and bounce away from the plates in a certain direction, breaking the cylindrical symmetry. The bounced off direction is beyond control but, nevertheless, it ignites DB at a neighboring point and subsequently in a series of DB points. The observed filament is formed by this continuous series of DB points. Furthermore, electroluminescence accompanies the DB and appears as a bright spot at the tip of the growing filament. Moreover, the heat and/or the chemical reactions produce bubbles (Figs. 20, 25 and 32) along the filament's growth path, and this pushes the fluid around and makes the situation more complicated.

The formation mechanisms of these filaments thus involve electrical, optical, fluid dynamics, heat transfer and chemical processes [Zaky & Hawley, 1973; Adamczewski, 1969], which are much more complicated than that found in most other pattern-forming systems (see Fig. 16). While a microscopic study is unavailable at this point, modeling at the *phenomenological* level presents itself. *And here enters active walks.*

For any filamentary growth, the filament can be viewed as the track left behind by an active walker. If we know how the walker changes its environment at every step, and how it picks its next step in the presence of this changed environment, then the track of the walker is determined. In the case of surface-reaction filaments under discussion, at each moment in time, the environment consists of the spatial distribution of the electric field, the temperature field, the densities of "unburned" and "burned" chemical fuels, the density and velocity distributions of the moving fluid, and the shape and location of the bubbles, not to mention the light intensity around the growing tip — the location of the active walker.

5.4.1. *Probabilistic active walk models*

The environment is indeed very complex. As a first approximation, we first represent the combined effect of all these influences in the environment by a scalar potential — the V in the AW model, then condense the complex dynamics of these influences and absorb them into the stochastic nature of a simple PAW (see Sec. 3.1). Using a W_1 landscaping function as a *fixed* template — i.e. the parameters in W_1 remain constant in the model, good agreements between the PAW and experimental results are obtained (see [Lam, 1997a] for a summary).

However, there are two outstanding problems. First, the dense winding pattern (Fig. 21) cannot be produced by a PAW. Second, the spontaneous morphological transition from radial wiggling to dense winding observed (Figs. 22 and 31) cannot be explained by a PAW using a fixed template. New AW models are needed.

(Note that in [Sheu *et al.*, 1999] the simulated pattern shown in their Fig. 3 is close packed, due to the use of six walkers, the short range influence represented by a small r_2, and branching. This pattern is *not* a dense winding pattern. A dense winding pattern is not just close packed, but consists of a *single* track without branching, winding back and forth around itself as the pattern expands as a whole in a certain direction (see Fig. 21). Secondly, the morphological transition shown in their Fig. 5 is *not* spontaneous. It is driven by the externally predetermined change of the parameter r_1, first increasing and then decreasing, as the distance from the starting point increases. See Sec. 5.4.2 for further discussion.)

5.4.2. *Thermal threshold active walk models*

A necessary condition for a close packed filament to form is that the "temperature" remains high enough around the recently created portion of the filament, so that the filament is favored to glow near its previous sections. In the simple fixed-template version of the PAW, this condition is achieved by adopting a small r_1 in the W_1 function (Fig. 6). Another trick is to allow a delay for the template to take effect, which may produce spiral patterns [Freimuth & Lam, 1992]. However, none of these methods are able to produce dense winding filaments. It seems we need a model for which the decay (through diffusion) of the temperature can be controlled.

The "Thermal Threshold Probabilistic" (TTP) model is such a model. The TTP model can work in any spatial dimensions. In particular, on a two-dimensional lattice, every site k has a temperature T_k. If the present location of the walker is at site i, let the set of empty sites j adjacent to i and with $T_j > T_h$, be denoted by B_i. Here the parameter T_h is the critical temperature (the subscript "h" stands for "heat," not site h); B_i is called the set of available sites. Every site j belonging to B_i may be

picked with the probability P_j, which is given by

$$P_j \propto (T_j - T_h)^\eta, \quad \text{if } T_j > T_h \tag{29}$$

and $P_j = 0$, otherwise. (See Fig. 33.) Then, m of these j sites are *actually* picked each time. After a site is picked, a new walker is placed there and heat is generated at this site, which then spreads out according to the diffusion law,

$$\chi \nabla^2 T = \frac{\partial T}{\partial t} \tag{30}$$

The temperature $T(\mathbf{r}, t)$ at any position $\mathbf{r}$ on this lattice at time t is the sum of the temperatures contributed by each of the early walkers. After the m walkers are added, the process is repeated.

Specifically, a walker created at time t_i at location $\mathbf{R}_i$ contributes a component $T_i(\mathbf{r}, t)$ to $T(\mathbf{r}, t)$ so that $T(\mathbf{r}, t) = \sum_i T_i(\mathbf{r}, t)$, with $T_i(\mathbf{R}_i, t_i) = A\delta(\mathbf{R}_i)$ and

$$T_i(\mathbf{r}, t) = \left[\frac{A}{4\pi\chi(t - t_i)}\right] \exp\left[-\frac{(\mathbf{r} - \mathbf{R}_i)^2}{4\chi(t - t_i)}\right] \tag{31}$$

which is the solution of the heat diffusion equation in two dimensions. Obviously, m is less than or equal to the maximum number of possible neighboring sites. For $m = 1$, there is no branching; branching occurs when $m > 1$. If the number of sites in the set B_i is less than m, we just pick all the sites in B_i.

In the TTP model, the four independent parameters are T_h, η, m and χ. Typical results from our TTP model, starting with a single walker at the center, are shown in Figs. 34–36. Good agreement between the TTP model and experiments are obtained.

To generate the dense winding pattern, it turns out that we have to add a bias in the overall growing direction of the pattern, the x direction in Fig. 37.

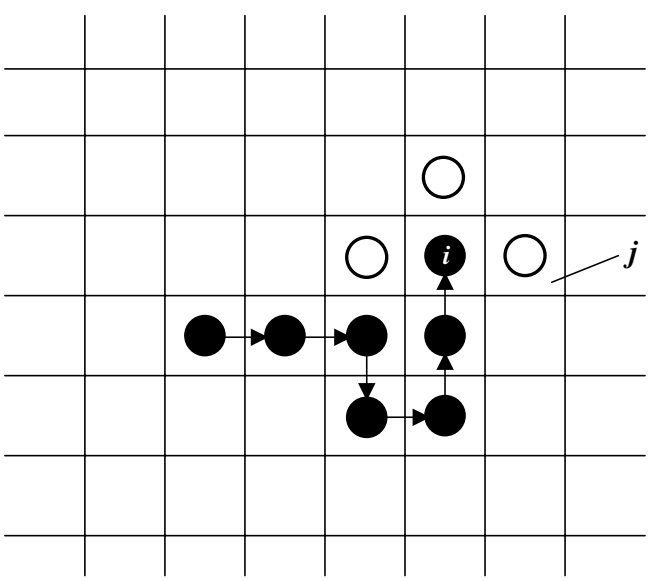

Fig. 33. Sketch of the "Thermal Threshold Probabilistic" (TTP) model. The positions of the active walker are represented by black dots. The three empty circles represent the empty sites adjacent to the current position of the walker at site i. The rule that the empty sites are picked is given in Eq. (29).

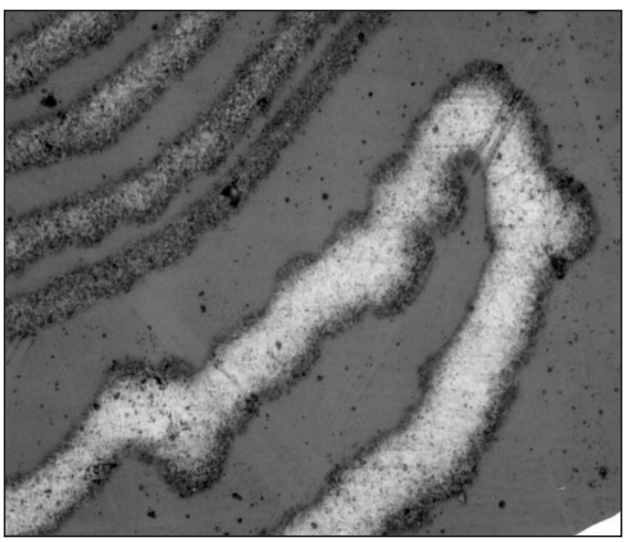

(a)

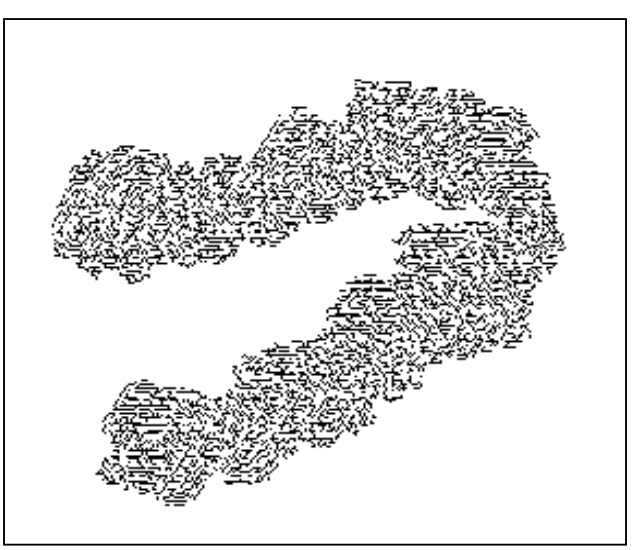

(b)

Fig. 34. (a) Experimental surface-reaction filament from an oil cell. (b) Simulation from the TTP model.

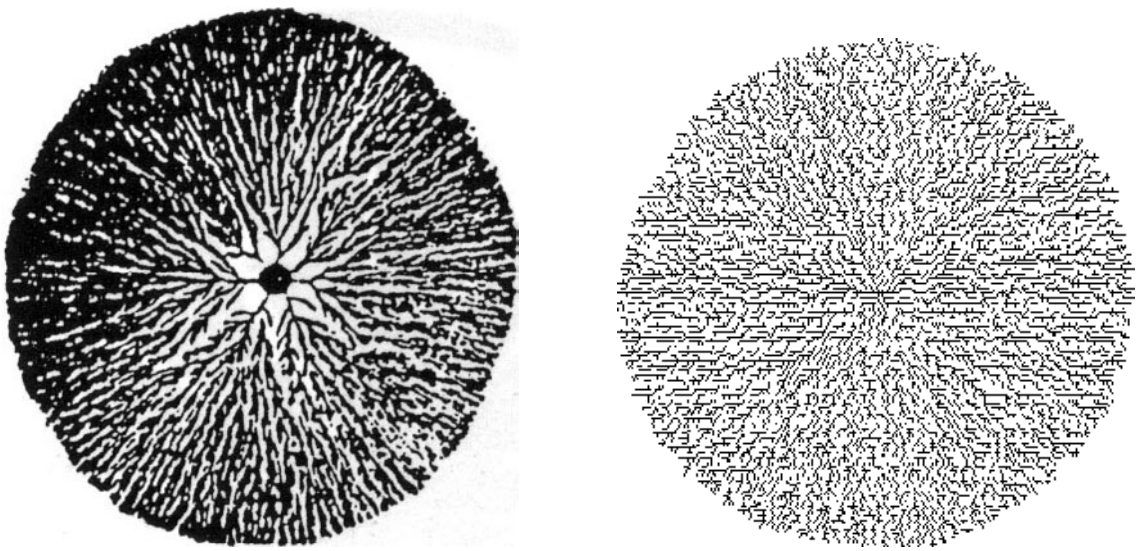

(a) (b)

Fig. 35. Dense radial morphology. (a) Experimental result from electrodeposit [Sawada *et al.*, 1986]. (b) Simulation from TTP model.

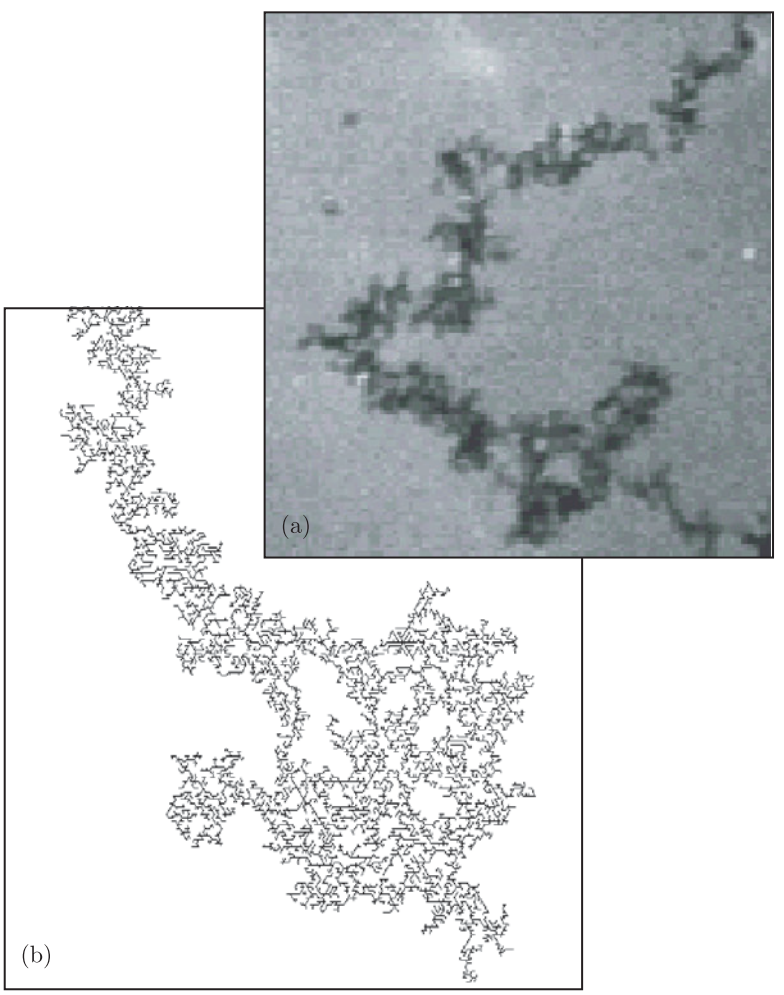

Fig. 36. Surface-reaction filaments. (a) Experimental result from an air cell. (b) Simulation from the TTP model.

The bias is added by giving a background temperature distribution in the form of a rising slope along the x direction. As can be seen in Fig. 37, the dense winding pattern is indeed reproduced.

To generate compact patterns, and filaments of finite or varying thickness (as shown in Fig. 1(b)), the "Thermal Threshold Aggregation" (TTA) model is created. In the TTA model, the set of available sites at each moment in time consists of *all* the perimeter sites (Fig. 38). m of these sites are picked with the TTP rule, and the process is repeated.

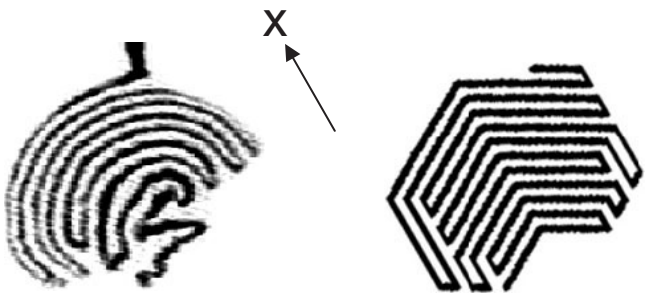

(a) (b)

Fig. 37. Dense winding pattern. (a) Experimental result. (b) Simulation from the TTP model, with a bias along the x axis. The bias is provided by a rising slope of temperature (of slope = 3) along the x direction. The parameters are: $\eta = 5$, $T_h = 5$, $m = 1$ and $\chi = 0.022$.

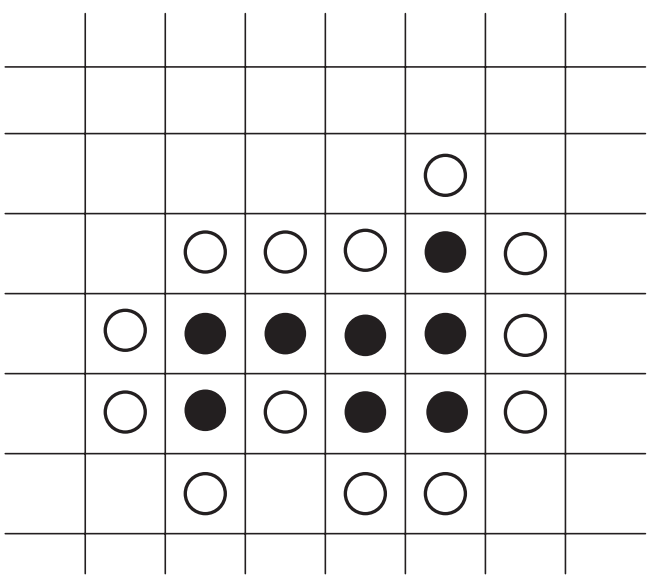

Fig. 38. Sketch of the "Thermal Threshold Aggregation" (TTA) model. The positions of the active walker are represented by black dots. All the perimeter sites, represented by empty circles, are available for picking under the rule of Eq. (29).

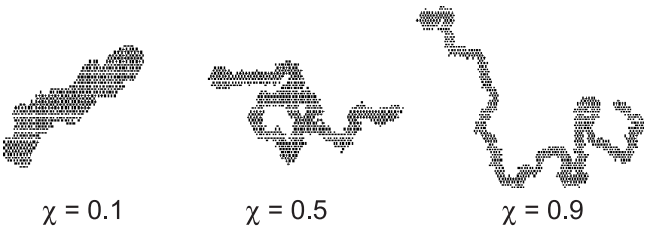

Fig. 39. Samples of filaments obtained from the TTA model.

Some results from TTA are presented in Fig. 39. Note that as the diffusion constant χ is increased, the temperature at the perimeter site decreases; less of them will have $T_j > T_h$ and be qualified to be picked. The aggregation filament is thus thinner.

In summary, the two thermal threshold AW models are more powerful and flexible than the fixed-template PAW model used before, with a lot of potential waiting to be explored.

Acknowledgments

I am grateful to the coauthors of my active walk papers. All of them were my students, except for Ru-Pin Pan and C. R. Sheu of the National Chiao Tung University in Taiwan, my coauthors in [Pan *et al.*, 1995]. While Richard Koepeke, Rocco Pochy, Michael Pon and Yuk Yung were M. S. students, the rest were undergraduates, namely, Lance Aberle, Jeffrey Fredrick, Rolf Freimuth, Daniela Kayser, Sue Ann Koay, My Phuong Le, Daniel Ratoff and Mike Veinott. An exchange undergraduate student from Germany, Michael Seifried, contributed to the research reported in Secs. 5.3 and 5.4.2.

References

Adamczewski, I. [1969] *Ionization, Conductivity and Breakdown in Dielectric Liquids* (Taylor & Francis, London).

Bachelier, L. [1900] "Théorie de la speculation," *Annales Scientifiques de l'Ecole Normale Supérieure* **III-17**, 21.

Baldassarri, A., Krishnamurthy, S., Loreto, V. & Roux, S. [2001] "Coarsening and slow dynamics in granular compaction," *Phys. Rev. Lett.* **87**, 224301.

Ball, P. [1999] *The Self-Made Tapestry: Pattern Formation in Nature* (Oxford University Press, Oxford).

Ben-Jacob, E., Schochet, O., Tenenbaum, A., Cohen, I., Czirók, A. & Vicsek, T. [1994] "Generic modeling of cooperative growth patterns in bacterial colonies," *Nature* **368**, 46–49.

Berry, B. J. L., Kiel, L. D. & Elliott, E. [2002] "Adaptive agents, intelligence, and emergent human organization: Capturing complexity through agent-based modeling," *Proc. Natl. Acad. Sci. USA* **99** (Suppl. 3), 7187–7188.

Bonabeau, E., Dorigo, M. & Theraulaz, G. [1999] *Swarm Intelligence*: *From Natural to Artificial Systems* (Oxford University Press, NY).

Buka, A. & Kramer, L., eds. [1996] *Pattern Formation in Liquid Crystals* (Springer, NY).

Cross, M. C. & Hohenberg, P. [1993] "Pattern formation outside of equilibrium," *Rev. Mod. Phys.* **65**, 851–1112.

Einstein, A. [1905] "Über die von der molekularkinetischen theorie der wärme geförderte bewegung von in ruhenden Flüssigkeiten suspendieten Teilchen," *Ann. Physik* **17**, p. 549.

Epstein, J. M. & Axtell, R. [1996] *Growing Artificial Societies* " (MIT Press/Brookings, Cambridge, MA).

Freidman, D. [2001] "Towards evoluation game models of financial markets," *Quant. Fin.* **1**, 177–185.

Freimuth, R. & Lam, L. [1992] "Active walker models for filamentary growth patterns," in *Modeling Complex Phenomena*, eds. Lam, L. & Naroditsky, V. (Springer, NY), pp. 302–313.

Gardiner, C. W. [1985] *Handbook of Stochastic Methods* (Springer, NY).

Helbing, D., Keltsch, J. & Molnár, P. [1997] "Modelling the evolution of human trail systems," *Nature* **388**, 47–50.

Huang, S. Y., Zou, X. W., Zhang, W. B. & Jin, Z. Z. [2002] "Random walk on a (2 + 1)-dimensional deformable medium," *Phys. Rev. Lett.* **88**, 056102.

Hughes, B. H. [1995] *Random Walks and Random Environments*, *Volume 1*: *Random Walks* (Clarendon, Oxford).

Katzenelson, O., Hel-Or, H. Z. & Avnir, D. [1996] "Chirality of large random supramolecular structures," *Chem. Eur. J.* **2**, 174–181.

Kauffman, S. [1993] *The Origins of Order*: *Self-Organization and Selection in Evolution* (Oxford University Press, NY).

Kayser, R. D., Aberle, L. K., Pochy, R. D. & Lam, L. [1992] "Active walker models: Tracks and landscapes," *Physica* **A191**, 17–24.

Kessler, D. A. & Levine, H. [1993] "Pattern formation in *Dictysostelium* via the dynamics of cooperative biological entities," *Phys. Rev.* **E48**, 4801–4804.

Lam, L. [1988] "Bowlic and polar liquid crystal polymers," *Mol. Cryst. Liq. Cryst.* **155**, 531–538.

Lam, L., Pochy, R. D. & Castillo, V. M. [1990] "Pattern formation in electrodeposits," in *Nonlinear Structures in Physical Systems*, eds. Lam, L. & Morris, H. C. (Springer), pp. 11–31.

Lam, L. [1991] "Unsolved nonlinear problems in liquid crystals," in *Nonlinear and Chaotic Phenomena*, eds. Rozmus, W. & Tuszynski, J. A. (World Scientific, Singapore), pp. 582–589.

Lam, L., Freimuth, R. D. & Lakkaraju, S. [1991] "Fractal patterns in burned Hele–Shaw cells of liquid crystals and oils," *Mol. Cryst. Liq. Cryst.* **199**, 249–255.

Lam, L., Freimuth, R. D., Pon, M. K., Kayser, D. R., Fredrick, J. T. & Pochy, R. D. [1992] "Filamentary patterns and rough surfaces," in *Pattern Formation in Complex Dissipative Systems*, ed. Kai, S. (World Scientific, Singapore), pp. 34–46.

Lam, L. & Pochy, R. D. [1993] "Active walker models: Growth and form in nonequilibrium systems," *Comput. Phys.* **7**, 534–541.

Lam, L. [1994] "Active walks," in *Lectures on Thermodynamics and Statistical Mechanics*, eds. Costas, M., Rodriqlulez, R. & Benavides, A. L. (World Scientific, Singapore), pp. 192–204.

Lam, L. [1995a] "Active walkers models for complex systems," *Chaos Solit. Fract.* **6**, 267–287.

Lam, L. [1995b] "Electrodeposit pattern formation: An overview," in *Defect Structure*, *Morphology and Properties of Deposits*, ed. Merchant, H. (The Mineral, Metals & Materials Society, Warrendale, PA), pp. 169–193.

Lam, L., Koepcke, R. W. & Lin, T. Y. [1995] "Active walks and soft computing," in *Soft Computing*, eds. Lin, T. Y. & Wildberger, A. M. (Society For Computer Simulation, San Diego), pp. 215–218.

Lam, L. [1997a] "Active walks: Pattern formation, self-organization, and complex systems," in *Introduction to Nonlinear Physics*, ed. Lam, L. (Springer), pp. 359–399.

Lam, L. [1997b] "Solitons: Integrable systems and non-integrable systems," in *Introduction to Nonlinear Physics*, ed. Lam, L. (Springer), pp. 211–271.

Lam, L. [1998] *Nonlinear Physics for Beginners*: *Fractals*, *Chaos*, *Solitons*, *Pattern Formation*, *Cellular Automata and Complex Systems* (World Scientific, Singapore).

Lam, L., Shu, C. Q. & Bödefeld, S. [1998] "Active walks and path dependent phenomena in social systems," in *Nonlinear Physics for Beginners*, ed. Lam, L. (World Scientific, Singapore), pp. 215–221.

Lam, L. [2000] "How nature self-organizes: Active walks in complex systems," *Skeptic* **8**, 71–77.

Lam, L. [2002] "Histophysics: A new discipline," *Mod. Phys. Lett.* **B16**, 1163–1176.

Lam, L., Koay, S. A., Le, M. P. & Yung, Y. [2002] "Active walk model for positive-feedback systems," *Workshop on Modeling Complex Systems*, Nov. 20–21, 2002, Reno, Nevada.

Lam, L. [2003] "Stochastic active walks and positive-feedback systems," in *Advances in Stochastic Structural Dynamics*, eds. Zhu, W. Q., Cai, G. Q. & Zhang, R. C. (CRC Press, Boca Raton, FL), pp. 287–292.

Marder, M. & Fineberg, J. [1996] "How things break," *Phys. Today*, September, pp. 24–29.

Maske, P., Havlin, S. & Stanley, H. E. [1995] "Modelling urban growth patterns," *Nature* **377**, 608–612.

Pan, R. P., Sheu, C. R. & Lam, L. [1995] "Dielectric breakdown patterns in thin layers of oils," *Chaos Solit. Fract.* **6**, 495–509.

Pelce, P. [1988] *Dynamics of Curved Fronts* (Academic, NY).

Pelce, P., Brujic, J. & Costier, L. [2004] *New Visions on Form and Growth*: *Dendrites*, *Flames*, *Fingered Growth and All That* (Oxford University Press, Oxford).

Pochy, R. D., Kayser, D. R., Aberle, L. & Lam, L. [1993] "Boltzmann active walker and rough surfaces," *Physica* **D66**, 166–171.

Ribotta, R. [1992] "Localized instabilities in the convection of nematic liquid crystals," in *Solitions in Liquid Crystals*, eds. Lam, L. & Prost, J. (Springer), pp. 264–292.

Risken, H. [1989] *The Fokker-Planck Equation* (Springer, NY).

Saffman, P. G. [1990] "Bubbles and fingers in Hele–Shaw cells," in *Nonlinear Structures in Physical Systems*, eds. Lam, L. & Morris, H. C. (Springer), pp. 3–10.

Savit, R., Manuca, R. & Riolo, R. [1999] "Adaptive competition, market efficiency, and phase transitions," *Phys. Rev. Lett.* **82**, 2203–2206.

Sawada, Y., Dougherty, A. & Gollub, J. P. [1986] "Dendritic and fractal patterns in electrolytic metal deposits," *Phys. Rev. Lett.* **56**, 1260–1263.

Schweitzer, F. & Schimansky-Geier, L. [1994] "Clustering of active walkers in a two-component system," *Physica* **A206**, 359–379.

Schweitzer, F., Lao, K. & Family, F. [1997] "Active random walkers simulate trunk trail formation by ants," *BioSyst.* **41**, 153–166.

Schweitzer, F. [1998] "Modelling migration and economic agglomeration with active Brownian particles," *Adv. Compl. Syst.* **1/1**, 11–37.

Schweitzer, F. [2003] *Brownian Agents and Active Particles* (Springer, NY). (Note: In this book, page 207, last line, "an electric field between the center and the boundary of a Hele–Shaw cell" should be replaced by "a vertical uniform electric field in a Hele–Shaw cell.")

Sheu, C. R., Cheng, C. Y. & Pan, R. P. [1999] "Dielectric breakdown patterns and active walker model," *Phys. Rev.* **E59**, 1540–1544.

Sheu, C. R., Cheng, C. Y., Wang, P. S., Lee, C. Y. & Pan, R. P. [2000] "Analysis of dielectric breakdown patterns in parallel-plate capacitors," *Chin. J. Phys.* (Taibei) **38**, 461–470.

Yuan, J. Y., Tremblay, B. & Babchin, A. [1999] "A wormhole network model of cold production in heavy oil," SPE 54097, *1999 SPE Int. Thermal Operations and Heavy Oil Symp.*, Bakerfield, CA, March 1999.

Zaky, A. A. & Hawley, R. [1973] *Conduction and Breakdown in Mineral Oil* (Peter Peregrinus, London).